

Infrared Image Super-Resolution: Systematic Review, and Future Trends

Yongsong Huang, *Student Member, IEEE*, Tomo Miyazaki, *Member, IEEE*, Xiaofeng Liu, *Member, IEEE*, and Shinichiro Omachi, *Senior Member, IEEE*

Abstract—Image Super-Resolution (SR) is essential for a wide range of computer vision and image processing tasks. Investigating infrared (IR) image (or thermal images) super-resolution is a continuing concern within the development of deep learning. This survey aims to provide a comprehensive perspective of IR image super-resolution, including its applications, hardware imaging system dilemmas, and taxonomy of image processing methodologies. In addition, the datasets and evaluation metrics in IR image super-resolution tasks are also discussed. Furthermore, the deficiencies in current technologies and possible promising directions for the community to explore are highlighted. To cope with the rapid development in this field, we intend to regularly update the relevant excellent work at https://github.com/yongsongH/Infrared_Image_SR_Survey.

Index Terms—Image Super-resolution, Deep Learning, Convolutional Neural Networks (CNN), Generative Adversarial Nets

I. INTRODUCTION

IMAGE super-resolution reconstruction (SR) is a classic low-level vision task in image processing [1]–[4]. The super-resolution reconstruction of IR images aims to recover high-resolution (HR) IR images from low-resolution (LR) IR images [1], [2]. Due to the existence of diverse degradation paths, the super-resolution reconstruction for IR images is still considered to be an ill-posed problem [2], [5], [6]. More details of the problem definition are shown in Eq. 1:

$$I_{LR} = \mathbb{D}(I_{HR}; \delta) \quad (1)$$

where \mathbb{D} denotes a degradation function, I_{HR} is the high-resolution IR image, I_{LR} is the low-resolution IR image and δ is the parameters of the degradation process. In general, the degradation process includes the following factors: 1) downsampling, 2) noise, and 3) compression, as shown in Eq. 2. In different real-world settings, the importance of these factors will be different.

$$\mathbb{D}(I_{HR}; \delta) = (I_{HR} \otimes \kappa) \downarrow_d + n_\varsigma, \{\kappa, s, \varsigma\} \subset \delta \quad (2)$$

where $I_{HR} \otimes k$ represents the convolution between a blur kernel k and the HR image I_{HR} . In the k , noise and compression are included. And, \downarrow_d is a downsampling factor, *e.g.*, $4\times$ and $8\times$. n_ς is some additive white Gaussian noise with standard deviation ς . Briefly, the super-resolution reconstruction objective function of IR images can be described as:

$$\hat{\theta} = \arg \min_{\theta} \mathcal{L}(I_{HR}, I_{SR}) + \lambda \Phi(\theta) \quad (3)$$

where \mathcal{L} denotes the loss function, between the HR image I_{HR} and the SR image I_{SR} . $\Phi(\theta)$ and λ are the regularization term and punishment parameter, respectively. Initial works follow the IR images SR as general image SR, and simply adopt the visible images SR model (*e.g.*, Convolutional Neural Networks (CNN)-based methods [7], Generative Adversarial Nets (GAN)-based methods [1], [8], [9], and transformer model [10]) to the new task.

However, it should be pointed out that the degradation process in infrared images is more complicated. The main reasons include the following: first, the blur kernel used in the reconstruction of visible images is relatively simple. It is typically Gaussian noise and JPEG compression [9], [11]–[14]. But, these blur kernels are not robust enough for IR images to represent complex real-world conditions. Because IR imaging systems are limited by optical physics and electronics. In other words, the noise generated is different. In addition, many IR cameras are deployed in the wild environment. It further increases the complexity of IR image degradation. On the other hand, the IR image presents simple color, insignificant gradients, and information overlap between high and low frequencies [11], [15]–[26]. These characteristics, which are different from visible images, can be considered to be unique patterns in IR images (see Sec.II-B). Consequently, it is necessary to propose super-resolution reconstruction approaches appropriate for IR images. We will discuss more details in future sections.

In this paper, we systematically review the applications, methods, and challenges in IR image super-resolution, targeting both academic researchers and industrial practitioners. This survey aims to bridge the gap between traditional SR methods and the unique characteristics of IR imaging, offering actionable insights for developing domain-specific algorithms. For academic researchers, it provides an in-depth analysis of innovative methodologies and open challenges. For industrial practitioners, it highlights practical challenges, such as hardware limitations and deployment in dynamic environments, with guidance for optimizing IR imaging applications in fields like autonomous driving, medical imaging, and remote sensing. By systematically analyzing existing approaches and identifying gaps, this survey serves as a foundational reference to advance research and practice in IR image super-resolution. Unlike other reviews, our survey focuses on recent deep-learning algorithms and summarizes the specific patterns used

This paper was produced by the IEEE Publication Technology Group. They are in Piscataway, NJ.

Manuscript received April 19, 2021; revised August 16, 2021.

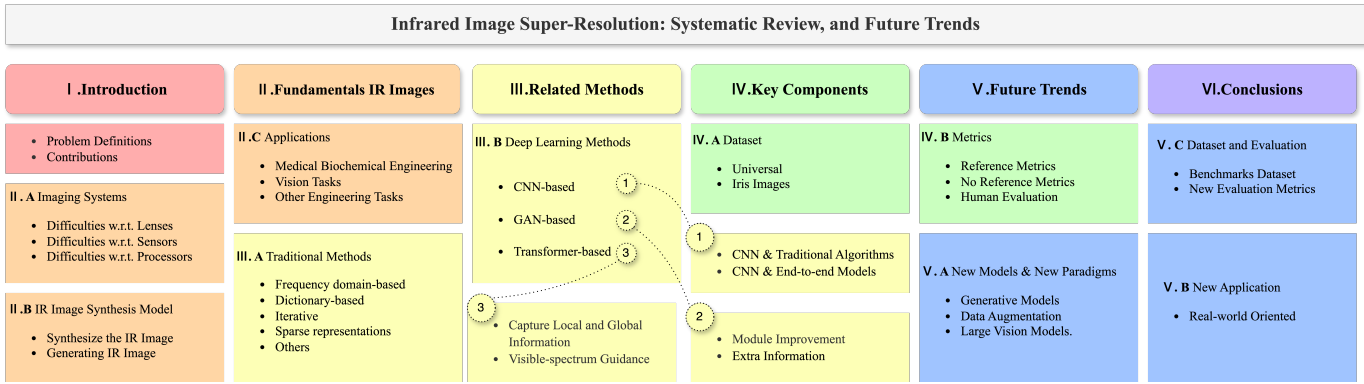


Fig. 1. Hierarchical and structural taxonomy of this survey.

in IR images for model representation. It will benefit the whole community to propose algorithms that are different from visible image reconstruction to improve the quality of IR images. To the best of our knowledge, this is also the first work that provides the most detailed explanation of why enhancing hardware systems to improve IR image quality is difficult. Unlike existing SR surveys [1]–[3], [27], [28], this survey uses the perspective of the IR image’s unique patterns to illustrate the challenges that distinguish it from visible images and also aims to review recent advances in SR techniques for IR images in the deep learning field. Meanwhile, we also summarized the application of IR images in various engineering fields. It will help the researchers to have a comprehensive insight into the entire field. The hierarchical and structural taxonomy of this survey is shown in Fig.1.

The left sub-figure in Fig.2 illustrates the evolution of methodologies for IRSR, categorizing them into traditional approaches, such as dictionary-based and frequency-based methods, and more recent deep learning-based techniques. Traditional methods dominated from 2000 to 2010, focusing primarily on frequency-domain modeling and sparse representation. Starting from 2011, the introduction of CNNs brought significant advancements, establishing their dominance for nearly a decade. More recently, GANs have emerged as a powerful tool for reconstructing high-quality textures, particularly excelling in applications requiring realistic detail synthesis, such as enhancing edges and textures in low-contrast IR images. However, their sensitivity to domain shifts often results in artifacts. In contrast, Transformer-based approaches [29], [30] excel in global contextual modeling, making them more robust for tasks requiring structural consistency and long-range dependency modeling, such as IR image reconstruction in dynamic environments. This progression highlights the continuous innovation in IRSR methodologies to address the unique challenges posed by IR images. Compared to traditional frequency-domain methods, which focus on enhancing high-frequency details, deep learning-based methods such as CNNs [31] and GANs [32] excel in learning non-linear mappings and synthesizing realistic textures. However, traditional methods remain advantageous in resource-constrained scenarios due to their lower computational complexity. Meanwhile, Transformer-based [29] and state-space models [33] bring

further advancements by enabling global contextual modeling and efficient scalability, making them particularly suitable for applications involving complex noise patterns and high-resolution requirements.

The right sub-figure presents the publication trends in the field of IRSR from 2000 to 2024. It demonstrates an exponential growth in research output, particularly from 2017 to 2024, where the number of publications rose sharply from 123 to 259. This surge reflects not only the technological advancements achieved through the adoption of deep learning-based methods, such as GANs and Transformers, but also the expanding practical applications of IR images in areas like autonomous driving, medical imaging, and remote sensing. These trends underscore the rapid evolution of IRSR research, making this survey a timely resource for researchers and practitioners aiming to navigate this dynamic field.

This survey’s contribution can be summarized as the following:

1) We systematically review the applications, methods, datasets, and evaluation metrics related to IR image super-resolution. In particular, we carefully investigated the application in IR image super-resolution using relevant methods since the beginning of the deep learning explosion. It includes the classification and summarization of these methods. 2) We also provide some unique pattern details in IR images that will benefit reconstruction, which are features making IR images super-resolution different from visible image super-resolution. It is common to see poor performance when directly transferring methods from visible images to IR images. It is promising to be solved by focusing more on the unique features of IR images. 3) We discuss trends, open issues, and challenges in IR image super-resolution. This section is dedicated to providing the community with new perspectives and new directions to explore. We will continue to update our open-source repository with new work in this area, and hope it will be useful for future highlighting research. The repository link is https://github.com/yongsongH/Infrared_Image_SR_Survey.

The remainder of this survey is organized as follows: Section 2 introduces the fundamentals of IR images and IR image applications; Section 3 describes image processing methods for IR image super-resolution in the literature; Section 4 presents the key components in IR image super-

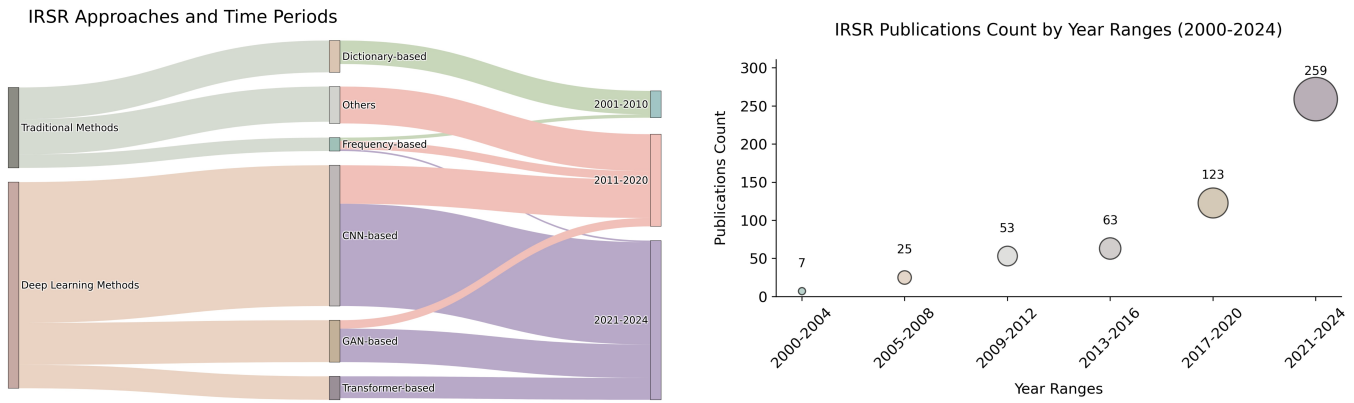


Fig. 2. [left sub-figure] Transition of IRSR methodologies across periods; [right sub-figure] Number of papers released to date. This analysis includes publications indexed in the Web of Science Core Collection from 2000 to 2024.

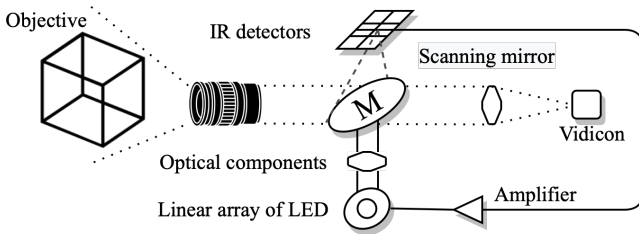


Fig. 3. Explanation of the operation mechanism in a FLIR system.

resolution: datasets and metrics; Section 5 discusses IR image specific patterns, future trends, and open issues; and Section 6 summarizes the work.

II. FUNDAMENTALS OF INFRARED IMAGES

In this section, we will introduce the fundamentals of IR images, which are IR imaging systems and applications. For the imaging system, we will discuss the components in the system and how these items influence the IR image quality. Then, the physics model of the infrared imaging quality limitation will be presented. Finally, IR image applications in different engineering fields will be classified and then discussed.

A. Imaging Systems

In the classical IR imaging system, the following basic components are included: lenses, sensors, processors, and others [2], [34]. In Fig. 3, we show the details in a classic forward-looking infrared (FLIR) system. On the linear array of IR detectors, the objective produces an image. Each detector’s amplified output drives a corresponding light-emitting diode (LED). After reflection from the back of the scanning mirror, this LED array is transferred onto an image tube (vidicon). In turn, this powers a typical cathode ray tube display. The whole system converts a scanned infrared image into a digital representation that can be seen on a monitor [34]. At present, the most popular infrared imaging systems use incorporate solid-state detectors.

We can achieve the goal, which is improving the IR image quality, by enhancing the performance of imaging systems.

According to current research, some key components in the imaging system: **lenses, sensors, and processors**, are significant in improving IR image quality. However, we will face many challenges in improving the image quality directly from the imaging system. More details will be discussed in the next sections.

1) *Difficulties w.r.t. Lenses*: In general, we need more light to be captured by the imaging system to get better image quality [34], [35]. But more light means a larger lens, which brings two main challenges: First, the more sophisticated instrumentation required will increase the costs and difficulties in the entire industrial design [36], [37]. Secondly, larger optical lenses make the size of the detector also larger [35]. It makes the whole size of the imaging system becomes larger and the combination of both becomes more difficult [38]. In motion situations, such as fast-moving environments, less light will arrive at the machine, making the image quality poor [35], [39].

2) *Difficulties w.r.t. Sensors*: With the captured IR light, the sensor is a key component to translate the light-wave signal to quantified signal. This component also involves two following major difficulties in improving the imaging performance. Firstly, there is the inherent noise of the sensor [40]–[44]. It is a noise called fixed pattern noise (FPN), which exists in the differences between bias voltages in column readout circuits of uncooled infrared sensors resulting in strong stripe noise which changes slowly in time [41], [45]. If we address this problem from hardware, it is almost impossible to solve it completely due to the physical limits [43], [46], [47]. Secondly, the limitation of device size makes it difficult for the current technology to make advances in the short term [35], [42].

3) *Difficulties w.r.t. Processors*: For many IR imaging systems, the traditional microprocessors are still equipped. Therefore, it may be difficult to run the sophisticated SR algorithms at the stage of image capturing, because of the limited computing power itself [46], [48].

Improving the performance of the equipment can be promptly expressed in the image quality improvement. However, as mentioned above, we will face many difficulties with the key components used in IR camera imaging systems. It

mainly includes the challenge of the fabrication process and physical limitations. For the fabrication process, we expect the camera to be more portable but often require larger lenses for better imaging. For processors, we need new technologies to improve computing and processing power, which requires more time and effort.

In summary, improving imaging quality from hardware will be costly in terms of industrial expense and effort, and the final performance improvement will be limited due to insurmountable physical obstacles. Next, another important task in IR imaging: synthetic models, will also be discussed.

B. IR Image Synthesis Model

In this section, we will discuss the IR image synthesis model in IR images. First, we will review previous work on synthesizing IR images. Then, the challenges of low-quality IR images that differ from normal images will be described. Finally, the connection between the IR image's unique patterns and the synthetic model will be presented.

1) *Synthesize the IR Image*: IR image quality relies on the proposed coloring physical model, which differs significantly from the normal image imaging in the visible wavelength band [49]. Briefly, the IR image color first requires the sensor to capture the radiance from the object, and then depends on the proposed coloring model. However, the IR image quality will be limited because of the heat transfer model or the coloring method is incomplete. Compared with normal images, which can be imaged by sensor capture with visible light, the influence from the heat transfer model or coloring approach is removed. In the following, the IR image synthesis method will be discussed.

Chanhee Oh's work pioneered the use of octree for precise IR imaging of objects, but it overlooked non-homogeneous materials and internal heat sources [50]. *Nandhakumar's* method addressed this by simulating internal heat source effects using a hierarchical Vs-tree model, but it struggled with complex shapes due to extensive node computations [51]. *Hyum-Ki Hong's* model represented heat transfer in non-homogeneous objects as an equivalent thermal circuit, effectively demonstrating the influence of the internal heat source [52]. However, it calculated surface radiance by only considering convection and internal heat source conduction, neglecting heat flow effects between adjacent facets.

It is clear that an effective IR image synthesis model must include all heat transfer modes inside the object, as well as the dynamic interactions between the object surface and its surroundings. With the help of these models, our goal is to capture the surface temperature variance to further generate IR images.

2) *Generating IR Image*: To generate IR images, we first required the surface radiance from the object and then generated the image according to the chosen coloring method. In this section, we will present a classical generation model based on atmospheric physics [49].

Atmospheric physics informs us that infrared radiation exhibits varying propagation characteristics at different wavelengths. In many spectral ranges, this radiation experiences

significant attenuation, rendering the source radiation detectable only within spectral ranges where the atmosphere is transparent, known as the atmospheric window. Consequently, when simulating infrared images of an object, object surface's radiance can be computed within this atmospheric window, utilizing *Planck's Law*.

The expression $e^{C_1/\lambda} \gg 1$ holds true within the infrared region, where λ is the wavelength: C_1 is the second radiation constant, $C_1 = 1.4388 \times 10^{-2} \text{ m} \cdot \text{K}$. Consequently, we can employ an approximation of *Planck's Law*:

$$E \approx \int_{\lambda_2}^{\lambda_1} \frac{C_1}{\lambda^5} e^{-C_2/\lambda T} d\lambda \quad (4)$$

Eq.4 represents the spectral radiant energy emission per unit time and per unit area from a blackbody at wavelength λ within the wavelength range $d\lambda$. Here, C_2 is the first radiation constant, with a value of $3.742 \times 10^{-16} \text{ W} \cdot \text{m}^2$. E denotes the spectral radiant emittance of a blackbody at an absolute temperature T .

By employing the partial integral method, we can approximate the evaluation of this integral as follows:

$$E \approx \frac{C_1}{C_2/T} e^{-C_2 X/T} \left\{ X^3 + \frac{3}{C_2/T} \left[X^2 + \frac{2}{C_2/T} \left(X + \frac{1}{C_2/T} \right) \right] \right\}_{X=\frac{1}{\lambda_2}}^{X=\frac{1}{\lambda_1}} \quad (5)$$

In the field of infrared image synthesis, high-quality IR images rely on a trusted heat transfer model first. This model requires a global estimate on the object's heat transfer state, both inside and on the surface of the object as well as the surrounding environment. Then, we further apply a pending radiance estimation method to calculate the radiance from the object. Finally the coloring model will color the image based on the radiance prior knowledge.

In accordance with *Wien's Displacement Law*, if $\lambda T < 3000 \mu\text{m} \cdot \text{K}$, the relative error introduced by Eq.5 is less than one percent. Upon determining the radiance of each surface patch using Eq.5, we compute the radiance of each vertex through interpolation. Ultimately, each surface patch is rendered using Gouraud Shading.

To summarize, the enhancement of IR images faces significant challenges, primarily due to hardware constraints arising from physical limitations and the complexity of image synthesis models. Further, we can summarize the unique patterns in IR images from the model used to generate these images:

- **Blur kernel.** The blur kernel employed in the reconstruction of visible images is comparatively straightforward, typically encompassing Gaussian noise and JPEG compression [9], [11]–[14]. However, these blur kernels lack the robustness required for IR images to accurately depict complex real-world scenarios or heat transfer model.
- **Degradation.** The deployment of IR cameras in uncontrolled, natural environments further exacerbates the complexity of IR image degradation.
- **Space information limited.** Because of the coloring model in IR image generating, the IR image presents simple color, insignificant gradients, and information overlap between high and low frequencies [11], [15]–[26]. Increased focus on these unique patterns will benefit to models applicable to IR images being proposed.

TABLE I
IR IMAGE SUPER-RESOLUTION APPLICATIONS.

Medical biochemical engineering	Vision tasks	Other engineering tasks	
Pharmaceutical industry [53], [54]	Image conversion [55]	Automated vehicle [56]–[58]	Food quality control [59], [60]
Medical science [61]–[64]	Multispectral matching [65], [66]	Remote sensing [67]–[71]	Agricultural management [72]–[78]
Cellular observations [79]–[81]	Targets detection [82]–[84]	Terrain models [69]	Water resource management [85]–[87]
Fluorescence microscopy [88]–[92]	Face recognition [93]–[97]	Land surface [70], [98], [99]	Star formation [100]–[103]

Based on the above concerns, we would resort to the subsequent image processing technology to improve the IR image quality. In the next sections, we will present IR image super-resolution methods, more economical, for applications in different fields.

C. Applications

IR image super-resolution reconstruction techniques have critical applications in various fields. In this section, we will show the applications in these key areas as shown in Tab. I. In summary, they can be generally divided into three categories: medical biochemical engineering, vision tasks, and other engineering tasks.

1) *Medical Biochemical Engineering*: For medical biochemical engineering, there are two typical examples presented here: neurodegenerative diseases and COVID-19 diagnosis. Super-resolution reconstructed infrared images can be used in the diagnosis of neurodegenerative diseases [61]. As a non-invasive examination approach, it helps to visualize and provide evidence for consultation. The current global epidemic COVID-19 diagnosis also requires the help of IR images. Because CT images are costly for large-scale population screening, the use of infrared imaging can provide a replacement. The super-resolution reconstructed IR images are also used to extract time-series features, which are finally used as a reference for classification using machine learning methods [62], [63]. Moreover, high-resolution IR images are fundamental for the visualization of living cells [79], [104], protein structure analysis [105], [106], and nanoscale drug [107]. These studies can be further developed with the help of super-resolution reconstruction in IR images.

2) *Vision Tasks*: For vision tasks, super-resolution reconstruction of infrared images also plays an important role. We will present several representative tasks: multispectral matching, image conversion, and object detection. Multispectral matching [65], [66] is popularly used in disaster prevention and homeland security. Better resolution of infrared images means better matching results. It is also beneficial for the object detection and other tasks. By using IR images, it is able to identify objects unaffected by the weather, illumination, or the environment’s color. And, image conversion can convert electro-optical (EO) images to IR images [55]. The image conversion is significant because we use IR images for recognition, but we often receive EO images. On the other hand, IR images are very critical for object detection in some environments. For example, penetrating IR images are the key information source after disasters such as earthquakes. With

the help of HR images, we can locate trapped people in dark environments, such as mines, by using localization algorithms [83], [108], [109].

3) *Other Engineering Tasks*: For other engineering tasks, we can find the value of high-quality IR images in different disciplines. In the automated vehicle, infrared images in low-visibility conditions would be beneficial for assisted driving systems, but high-resolution thermal imaging sensors are typically expensive, which limits the general availability of such imaging systems [56]. Therefore, super-resolution techniques can be used to improve performance in this field [110], [111]. Further, super-resolution IR images have the potential to provide substantial improvements to interferometric observations of protoplanetary disks [112]. Moreover, estimates of relative dust optical depth and source brightness are also important [101]. Ultra-high-resolution IR images are also needed in the study of ongoing star formation [113], [114]. Applications in other domains can be found in more detail in Tab. I.

III. RELATED METHODS

In this section, we will introduce IR image super-resolution methods, including traditional methods and deep learning-based methods. For the traditional algorithms, there will be three parts: frequency domain-based, dictionary-based, and other methods. Then, the deep learning methods will be presented.

Fig.4 provides a chronological overview of representative IRSR algorithms, illustrating the key advancements in this field from 2000 to 2024. The timeline highlights how traditional methods, such as frequency domain-based approaches and dictionary learning algorithms [115], laid the foundation for early IRSR research. These methods, prevalent from 2000 to 2010, primarily focused on mathematical models and hand-crafted features to enhance IR image quality [116]–[118]. However, they often faced limitations in handling complex noise patterns [119] and adapting to diverse real-world scenarios. This paved the way for the adoption of deep learning approaches, starting in 2011, particularly CNN-based methods [120]. By learning hierarchical feature representations, these methods achieved significant improvements in reconstruction quality and robustness, marking a turning point in the development of IRSR techniques.

In recent years, GANs and Transformer-based models have pushed the boundaries of IRSR methodologies even further. GANs, introduced around 2018, enabled realistic texture generation, effectively addressing the unique noise characteristics

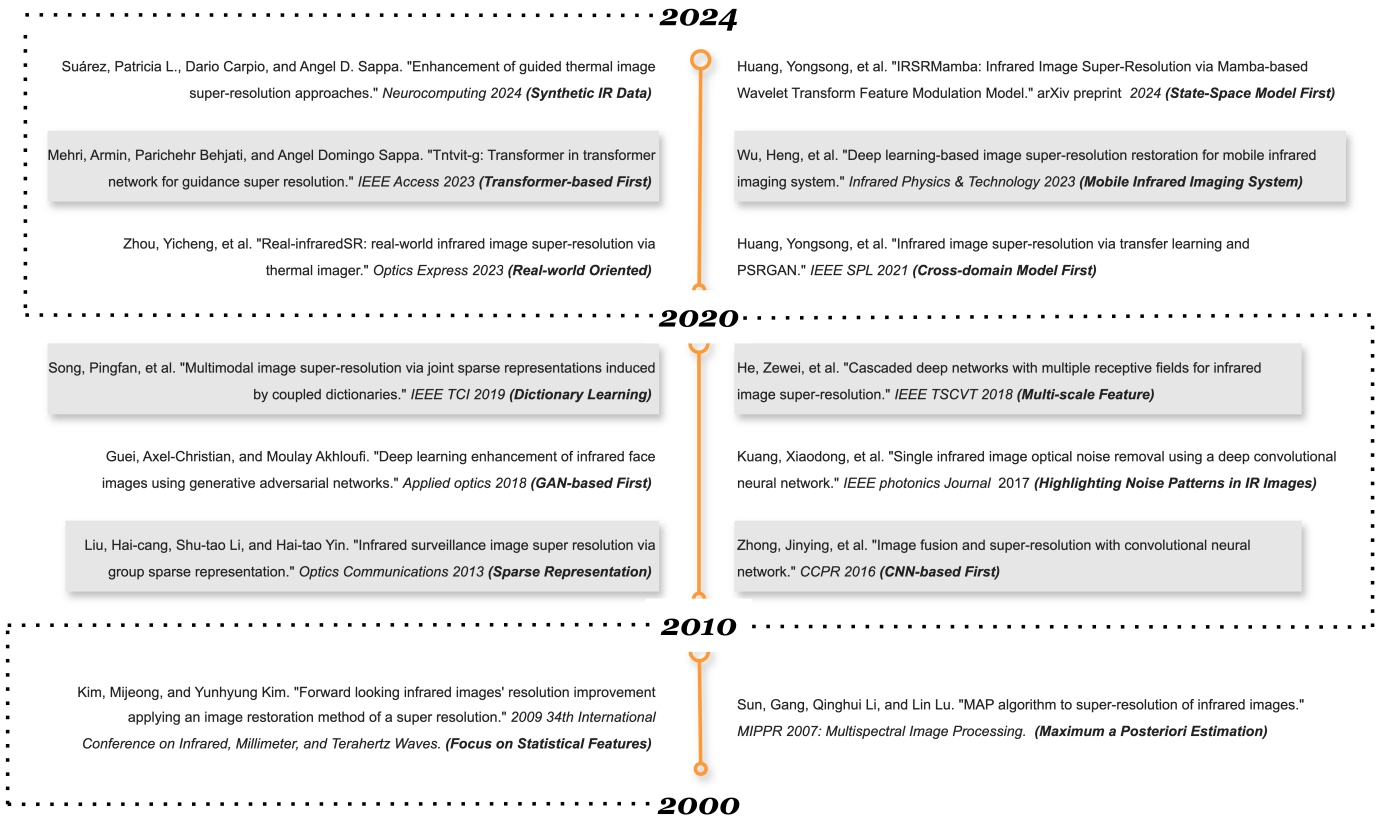


Fig. 4. The timeline of representative IRSR algorithms (from year 2000 to 2024).

of IR images [121]. Meanwhile, Transformer-based models, exemplified by recent works such as [29], have enhanced global contextual modeling capabilities, resulting in superior performance in preserving structural consistency and fine details. This evolution reflects a broader trend toward leveraging advanced deep learning architectures to overcome the inherent challenges of IRSR. Additionally, recent studies have extended the scope of IRSR by exploring cross-domain learning [122], mobile infrared imaging systems [123], and state-space modeling [33], demonstrating the growing practical relevance and applicability of these techniques.

Based on the advancements in IR imaging systems and deep learning techniques, researchers are increasingly focusing on developing more efficient image processing methods to enhance IR image quality further. As such, this survey categorizes image processing approaches into two primary types: traditional methods and deep learning-based techniques. To provide a clear comparison, Table II lists several representative works, summarizing their performance and contributions. This comparison not only highlights the progress made in the field but also underscores the evolving role of deep learning in addressing the specific challenges of IR image super-resolution.

A. Traditional Methods

In traditional image processing algorithms, the IR image super-resolution follows the direction of visible image super-resolution. Specifically, these approaches include **frequency domain-based, dictionary-based, and other methods.**

1) *Frequency Domain-based*: For the frequency domain-based approach, we will decompose the IR image into two domains: the air domain, and the frequency domain [135]. Especially for multiple complex frequency domain components, it is often not included by a simple FFT. For example, there is a significant difference between high-frequency and low-frequency information in IR images. *Choi et al.* propose a new frequency-domain processing method for this problem: firstly, the edge pixels are distinguished, then the high-frequency information is enhanced independently, and finally, a high-resolution image is available [136].

$$e(\hat{k}, l) = \left(1 - e^{-\frac{(\lambda_1 + \lambda_2)}{\sigma_{\text{sum}}}}\right) \left(1 - e^{-\frac{(\lambda_1 + \epsilon)/(\lambda_2 + \epsilon)}{\sigma_{\text{ratio}}}}\right) \quad (6)$$

As shown in Eq. 6, the researchers introduced prior knowledge skillfully. Two eigenvalues are denoted by λ_1 and λ_2 , where $\lambda_1 \geq \lambda_2 \geq 0$, which are recalculated from the structure tensor at pixel (\hat{k}, l) , σ_{sum} and σ_{ratio} indicate established parameters. In order to avoid division by zero, a tiny constant named ϵ is created. It is important to mention that we will need a carefully engineered prior with expert knowledge to ensure the performance, which is difficult to achieve with the current relatively weak physical modeling [2]. On the other hand, there are also some frequency domain-based methods focusing on the reconstruction time issue and aiming to accelerate [137]. Because we will fuse 4 images to get better image resolution.

TABLE II

PERFORMANCE COMPARISON [IN TERMS OF PSNR (dB) AND SSIM] OVER SELECTED TEST DATASET FOR 4 OR 3 UPSCALING FACTORS. SOME OF THESE WORKS USE VISIBLE IMAGES [124] AS TRAINING DATASETS, SUCH AS 7 AND 9. THE TEST DATASETS FOR THESE REPRESENTATIVE METHODS DEPEND ON THE TASK, CHECK THE REFERENCES FOR MORE DETAILS.

No.	Methods	Year	Ref. \times 4 (PSNR/SSIM)	Keywords
1	Wu, Wenhao, et al. [125]	2022	31.69/0.7877	Meta-learning; Lightweight network
2	Huang, Yongsong, et al. [122]	2021	33.13/0.8282	Transfer learning; Small sample
3	Liu, Qing-Ming, et al. [126]	2021	32.23/0.8720	Attention mechanism; GAN
4	Prajapati, Kalpesh, et al. [14]	2021	34.90/0.9134	Attention mechanism; Channel splitting
5	Marivani, Iman, et al. [127]	2020	35.19/0.9888	Sparse coding; Image fusion
6	Marivani, Iman, et al. [26]	2020	34.49/0.9853	Multimodal image; Residual learning
7	Yao, Tingting, et al. [128]	2020	34.54/0.8807	Dictionary learning; CNN
8	Song, Pingfan, et al. [115]	2020	36.36/0.9796	Dictionary learning; Sparse representations
9	Batchuluun, Ganbayar, et al. [129]	2020	22.99/0.9760	Image deblurring; GAN
10	Rivadeneira, Rafael E, et al. [130]	2019	37.85/ \emptyset	Thermal images; CNN
11	Suryanarayana, Gunnam, et al. [19]	2019	31.40/0.9513	Discrete wavelet transform; CNN
12	Marivani, Iman, et al. [131]	2019	33.19/ \emptyset	Sparse coding; CNN
13	He, Zewei, et al. [132]	2018	36.02/0.9230	Multiple receptive fields; CNN
14	Sun, Chao, et al. [133]	2018	32.71/ \emptyset	Zoom mechanism; Transfer learning
15	Han, Tae Young, et al. [25]	2018	39.69/0.9582 (\times 3)	Frequency components; CNN
16	Zhao, Yao, et al. [134]	2016	30.69/0.9031 (\times 3)	Compressed sensing; Dictionary learning;

In addition, since the edges of the original image are bold, it will be difficult to match the edges during registration.

2) *Dictionary-based*: Considering the good interpretability, the dictionary-based reconstruction methods have gained a lot of popularity among researchers in IR images. The formalization of the dictionary-based reconstruction method can be found in this work [138]. In summary, the dictionary-based approach focuses on patches that build a bridge between I_{HR} and I_{LR} . These patches include features such as **1)** correspondence, **2)** the number of patches, and **3)** inter-patch relationships. The correspondence relationship and the number of patches are used to ensure that the mapping between the I_{LR} and the I_{HR} is complete. And the patterns of the low-resolution image can be preserved in the high-resolution image by the inter-patch relationship. The proposed methods improve the image quality from these perspectives, and more details are shown in Tab. III.

We will briefly describe the representative dictionary-based works: **First, dividing the groups**. On the one hand, it has been observed that the similarity between image groups impacts the reconstruction, that is, similarity and compatibility as previously discussed. This approach considers group similarity and proposes positional constraints. The position between groups is used as a feature to constrain the reconstruction of the image [139]. In addition, multiple information (multi-view) is introduced to reconstruct images using more groups to represent instead of isolated groups [140], [141]. Researchers use multi-scale groups to compile dictionaries, which can provide rich scale information and diverse structural information [141]. In specific tasks, such as pedestrian recognition, if the person as a target is segmented into different blocks will hurt the recognition results. In this situation, multi-scale

blocks can keep the person retained in the complete block while further constructing the dictionary [142]. **Second, the relationship between the total number of dictionaries and reconstruction**. The researchers dropped the question that the single dictionary created from IR images has limited the development of dictionary-based methods or not. This limitation is expressed in two directions: fewer dictionary pairs and less information about the IR images. It is proposed that a single dictionary cannot represent all the structural information. And, multiple dictionaries should be used to support the reconstruction [143].

$$\begin{aligned}
 \mathbf{x}^h &= \Psi_c^h \mathbf{z} + \Psi^h \mathbf{u}, \\
 \mathbf{x}^l &= \Psi_c^l \mathbf{z} + \Psi^l \mathbf{u}, \\
 \mathbf{y} &= \Phi_c \mathbf{z} + \Phi \mathbf{v}.
 \end{aligned} \tag{7}$$

Moreover, it is also the first time that extra dictionaries are constructed using visible image information obtained from the same scene in a dictionary-based approach to help the reconstruction. **Third, the information, from other types of images, can also be used to support the dictionary construction**. Because the image information in the IR image itself is insufficient due to the poor imaging environment. Then, people started to focus on introducing extra information. This algorithm is developed to enhance the resolution of the target LR image with the aid of another guidance HR image modality [115]. More details are shown in Eq. 7.

They express the LR image patch $\mathbf{x}^l \in \mathbb{R}^M$ and HR image patch $\mathbf{x}^h \in \mathbb{R}^N$ of the same image modality, and the guidance HR patch of another different image modality $\mathbf{y} \in \mathbb{R}^N$. The definitions of the symbols can be found in Abbreviations and

TABLE III
DICTIONARY-BASED RECONSTRUCTION METHODS.

Category	Method	Key idea
Patches	Cheng-Zhi, Deng, et al. (2014) [139]	Considering the similarity between groups, the locality-constrained group is proposed to guide the reconstruction by using the positions between groups as features.
	Yang, Xiaomin, et al. (2015) [140] Yang, Xiaomin, et al. (2017) [141]	Introduce multi-view information and multiscale information to build patches.
	Yang, Xiaomin, et al. (2016) [143]	Using more dictionaries.
Dictionary	Yang, Xiaomin, et al. (2016) [143]	Using more dictionaries.
	Yao, Tingting, et al. (2020) [128]	It is proposed to capture more IR image features with neural networks and then use this information to build dictionaries.
Correspondence Relationship	Zou, Erbo, et al. (2018) [142]	To better represent the pattern of groups, this work improves performance by learning the correspondence several times.
Extra Information	Song, Pingfan, et al. (2019) [115]	Other image modalities, such as RGB images, are introduced to enhance edge and structure primitives information.
	Chen, Zuming, et al. (2018) [145] Wang, Yan, et al. (2021) [144]	These works propose to pay more attention to the gradient information in IR images.

Notations. Some works noticed that gradient information of IR images would be beneficial for reconstruction [144], [145].

3) *Other Traditional Algorithms*: There are other traditional algorithms used for IR image super-resolution listed here, as shown in Tab.IV. Some methods aim to transfer the super-resolution methods in visible images to IR images. **1) Iterative** methods are used in some biometric application situations, such as iris recognition [146], and laser line scanning thermography [147]. However, such methods are not fine-tuned according to the special patterns in IR image. **2) Sparse representations** are used in land remote sensing where the IR term with IR information is calculated by computing the normalized difference target index (NDTI). There are also swarm optimization algorithms applied to minimize the terms to get the land cover target mapping (LCTM) [15]. **3) In sparsity-based methods**, researchers pay more attention to the specific patterns in IR images. In such methods, it is still common to process information in the frequency domain. However, if we only consider the frequency domain, the contribution from the space domain information may be ignored. For example, the similarity between neighboring points is considered, different from the general frequency domain-based approach, where the image gradient represented by sparsity is mentioned [20], [22]. In addition, there are new directions, *i.e.*, using higher-order image derivatives to receive the image prior to sparsity [148], [149].

S. C. Park et al. described the details about the **projection method** in his work carefully [2]. Such methods require appropriate priors to guide the projection, and researchers considered the phase characteristics in images to improve the algorithm [21]. It is also proposed to introduce illumination sensitivity prior to construct iterations [150].

On the other hand, **regularization** methods also play a key role. *Yu Hui et al.* [151] believed that the regularization term can also suppress the unnecessary low-frequency components and enhance the image quality. A two-step fully-variable sparse reconstruction algorithm is designed by *Wang et al.* [15] The fully-variable regularization term is added to the classical compressed perceptual model.

TABLE IV
IR IMAGE SUPER-RESOLUTION VIA OTHER TRADITIONAL ALGORITHMS.

Category	Method
Iterative	A. Fernandez, et al. (2017) [146] Ahmadi, Samim, et al. (2020) [147]
	Wang, Peng, et al. (2021) [154]
Sparsity	Liu, Xingguo, et al. (2019) [22] Güngör, Alper, et al. (2019) [20] Liu, Xingguo, et al. (2018) [148] Chen, Shaojun, et al. (2019) [149]
	Zhang, X. F., et al. (2019) [21] Liu, Jinsong, et al. (2016) [150]
	Yu, Hui, et al. (2013) [153] Hui, Yu, et al. (2014) [151] Wang, Yan, et al. (2022) [15]

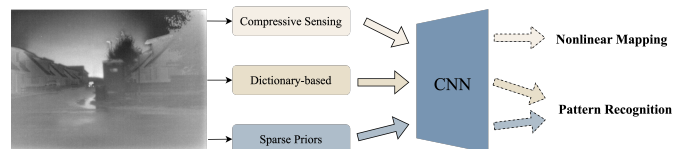


Fig. 5. CNNs contribute to other traditional methods used to learn nonlinear mappings and pattern recognition.

The weaknesses in such methods are also easily observed in experiments: *Dijk et al.* mention that regularization methods influence the performance in detection tasks [152]. Moreover, it is supposed that the model is not considered for complex nonlinear degradation factors. The result is that algorithms have limited fitness for real-world applications [153].

B. Deep Learning Methods

With the development of deep learning, neural networks have shown remarkable performance in image super-resolution

TABLE V
CNN TRANSFERS ON TRADITIONAL METHODS.

Category	Method	Highlight
Compressive Sensing	Zhang, Xudong, et al. (2018) [23]	Nonlinear Mapping
Dictionary-based	Yao, Tingting, et al. (2020) [128]	
Sparse Priors	Marivani, Iman, et al. (2020) [127]	Pattern Recognition

with powerful fitting ability [7], [8], [155]–[158]. However, few previously published studies have been able to draw on any systematic research into IR image-specific patterns. These unique patterns include gradient information, high or low-frequency information, extra information, etc [21], [64], [122], [159], [160]. In this section, we will also focus on the differences between IR images and visible images in the deep learning field of super-resolution. In summary, the challenges of IR image super-resolution in deep learning include specific patterns, difficulty in representing patterns, and poor image quality. More details will be shown in the next section.

1) *CNN-based*: There are two major trends for CNN-based models in IR image super-resolution: **1)** First, researchers introduced CNNs as contributors to improving traditional algorithms (see Fig. 5, Tab.V). **2)** Further, it became popular to use CNNs to build end-to-end models used in IR image super-resolution.

CNN & Traditional algorithms: As mentioned in Sec .III-A, traditional methods require enough prior knowledge to achieve image super-resolution. However, weak mathematical analysis limits the proposed algorithms. CNN can learn nonlinear mappings without indication because of its powerful fitting ability [7], [8], [155]–[158]. It allows people to free themselves from the task to seek for priors. Initially, neural networks were not used to reconstruct IR images directly. Rather, it was carefully used to help traditional algorithms improve performance through **nonlinear mapping and pattern recognition**.

1) *Nonlinear mapping*: In infrared camera systems, there will be little high-frequency information and low-frequency information in the captured infrared image compared to the visible image due to the poor imaging environment (see Sec.II-A). It becomes a challenge to better represent these two kinds of information in IR images super-resolution. Then, the researchers proposed that CNN can be used to represent the nonlinear mapping of low and high frequency information in the latent space. In *Zhang’s work* [23], the SR image is reconstructed using compressed sensing first. Then the SR image and HR image are reduced to receive high-frequency noise information. Finally, the information is fed into CNN to learn nonlinear mapping.

$$\mathcal{L} = \frac{1}{2N} \sum_{i=1}^N \|\tilde{R}(\Theta, i) - R(\Theta, i)\|^2 \quad (8)$$

Eq.8 denotes the loss function to learn the trainable parameters Θ in CNN. Corresponding to i th training image, $\tilde{R}(\Theta, i)$ represents the estimated residual image produced by CNN, while $R(\Theta, i)$ represents the true residual image used

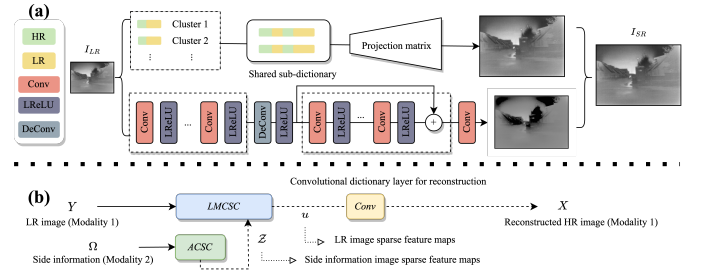


Fig. 6. (a) shows the CNN used as a feature extractor in a dictionary-based approach; (b) is an illustration for the CNN used to represent prior.

for training [23]. Experiments show that this approach using CNNs to represent nonlinear mappings for reconstructing IR images can enhance detailed information.

2) *Pattern recognition*: On the other hand, *Yao, Tingting, et al.* [128] proposed to use CNN as a feature extractor in the dictionary-based approach. This method also focuses on the problem that the detailed information in IR images is important, and CNN can build the dictionary with more details added to the representation. Novel interpretable operators are proposed to construct the basic module as the sparse representation for prior extraction, another module to represent the edge information of visible images, and finally fused in a residual network using skip connection [127].

More details are shown in Fig.6. For (b), X and Y denote the LR image, and reconstructed SR image, respectively. The convolutional sparse codes Z of the guidance HR image Ω are similar to u by means of the ℓ_1 -norm according to the literature [127]. Furthermore, residual networks with multiple branches are used to reconstruct high and low-frequency information, respectively [17].

Beyond introducing CNNs, these existing methods started to introduce visible images to guide the reconstruction of IR images purposefully, which represents an entirely new direction. Further, attention has been focused on image characteristics, specifically the difference between high and low-frequency information in IR images. Details will be described in the next sections.

CNN & End-to-end models: In this section, the end-to-end models used in IR image super-resolution will be presented. The high-frequency and low-frequency information in IR images is responsible for the image outline and edges, respectively. Moreover, the IR image has less edge information compared to the visible image because of the imaging system (see Sec.II-A). **First, the researchers propose that the independent extraction for high-frequency and low-frequency information in IR images is achieved by CNN.** In [161], *Zou et al.* used residual networks to build a model similar to U-Net. The multi-receptive field module in this work is supposed to help represent the features of high and low-frequency information. Similar work is [160], and the residual network is also used. However, the information distillation approach is used in the backbone network, which was first proposed in [122] to benefit IR image super-resolution. This Information distillation-based model is also considered to be helpful for different information extraction. In addition, *Kwasniewska et*

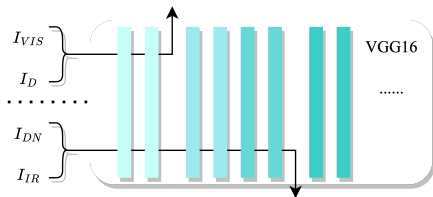


Fig. 7. I_{DN} denotes the denoised output, while I_D is the output from the author’s proposed network [17].

TABLE VI

ABLATION STUDIES FOR INTRODUCING VISIBLE IMAGE INFORMATION. FROM 1 TO 4 STARS, INDICATES THAT THE SUBJECTIVE EVALUATION IS IMPROVING.

Residual Network	✓	✓	✓	
Visible Images (Training Dataset)		✓	✓	✓
Novelty Loss			✓	✓
Novelty Network				✓
Results	*	**	***	****

al. used a wide receptive field residual network constructed by dense connection [162]. According to the experimental results, this work confirmed that wide receptive fields are effectively used for low-contrast images. *Prajapati, Kalpesh, et al.* suggest that the common residual design allows for retaining too many redundant features in the network. A new module for integration with multiple attention mechanisms is proposed in their work. According to the experimental results, this novel attention mechanism module will help to enhance the high-frequency information representation [14]. Finally, not only the residual network is used, but also the importance of edges is observed [11]. The method that enhances high-frequency details and contacts information-tail modules to improve details is the highlight. More details are shown in Fig.8. And F_{nlm^D} is the output of the previous (*i.e.* D) recursive block

The approaches mentioned above show that the two variables in the latent space (low-frequency and high-frequency information) are treated independently. Then novel methods are used to represent the nonlinear mapping between these two independent variables respectively. **In the next section, we will describe another category of methods that introduce extra information: visible image information (see Tab.VI).**

For introducing visible image information, the researchers focused on the following components: dataset, network structure, and loss function. It is natural to associate using visible images to train neural networks because they are cheap and easy to use, with rich detailed information. However, it is difficult to fit the data distribution for IR images with the model trained on the visible image dataset due to the domain transfer challenge [122], [130]. In other words, the SR images have poor quality. Then, adaptations to the loss function are proposed. As we all know, the loss function is important for optimizing neural networks. *Patel, Heena M., et al.* proposed that a combined loss function, with two terms for L1 and SSIM loss, could be used [163]. According to the ablation

experiments, this combined loss function would be beneficial for their proposed improved dense blocks. On the other hand, it also inspired that appropriate loss functions would be useful for introducing information from visible images In [17], the authors propose that the perceptual similarity between IR images I_{IR} and paired visible images I_{VIS} can be captured by CNNs. And there are features present in the middle layer of the neural network and they can be used as loss functions (see Fig.7).

Next, we will introduce novel network structures for using visible image patterns. *Zou, Yan, et al.* proposed a dual-path residual network that directly fuses the features from visible and IR images in the channel [164]. Further, *Oz, Navot, et al.* consider that dimensionality compression will influence the performance in feature fusion. Because the correlation between adjacent pixels is ignored. Then, the dimensional change network for increasing channels was proposed [165].

Finally, we will also present models related to super-resolution in multi-vision tasks. In many vision tasks [120], [166], such as segmentation and fusion, super-resolution is applied to help other subjects as a pre-processing task. In particular, the regression network proposed in [166] is dedicated to prevent the irrelevant function mapping space on the reconstructed images by using forward generation and backward regression. This double mapping constraint is used for IR image super-resolution, and then the output that has better image quality is used in the fusion task. More details can be found in Fig.9.

The loss function used in this work is: x_i and y_i respectively represent the LR image I_{LR} and output SR images I_{SR} . $\mathcal{L}_1(F(x_i), y_i)$ and $\mathcal{L}_2(D(y_i), x_i)$ describe the loss functions of forward regression and inverse regression tasks, respectively.

$$\mathcal{L} = \sum_{i=1}^N \mathcal{L}_1(F(x_i), y_i) + \lambda \mathcal{L}_2(D(y_i), x_i) \quad (9)$$

Moreover, this work mentions that intensity distribution and gradient information can represent thermal radiation and structural information, separately.

In summary, the approaches in IR images and CNNs have first tried to combine the pattern recognition capabilities of CNNs into traditional reconstruction methods, such as dictionary reconstruction and sparse coding. Then started to reconstruct IR images directly using end-to-end models. Many module-based improvement methods were proposed, such as multi-scale information extraction. However, the high and low-frequency information in IR images have a significant gap. To use this information, the model structure has been improved further, for example, by presenting the information separately in different modules or using more complex modules. Compared to IR images, visible images have information with rich details. For this reason, researchers have started to try to use visible images to help reconstruct IR images. It includes designing new network structures and using strategies such as transfer learning. The purpose is to help neural networks can introduce more patterns and information from visible images.

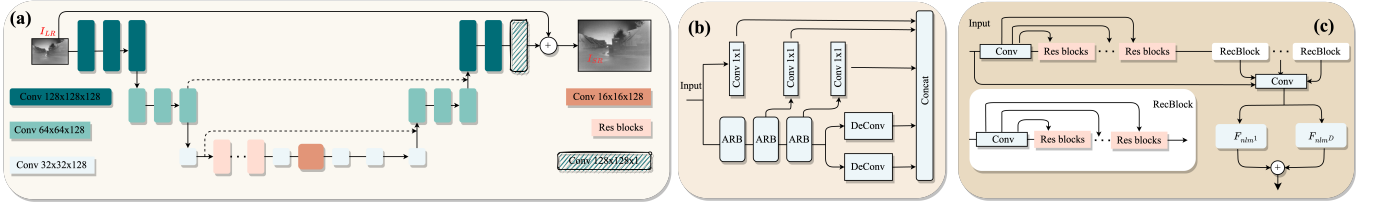


Fig. 8. In (a), the researchers used a network similar to U-Net to extract high and low-frequency information independently [161]. For the same purpose, (b) demonstrates that the information distillation method can also be used [162]. Finally, the module in (c) shows that wide receptive fields are beneficial for low-contrast images [11].

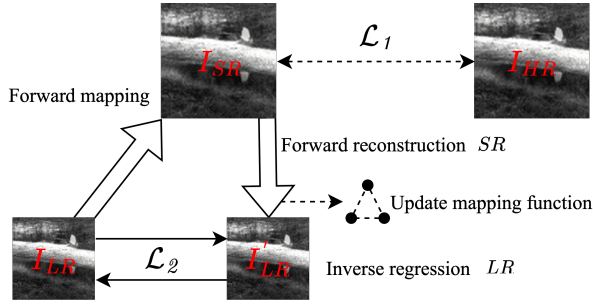


Fig. 9. Regression network structure.

2) *GAN-based*: After GAN [167] was proposed, research based on adversarial training model is emerging in the super-resolution field. SRGAN [8], ESRGAN [158], and various other types of GAN models [168] moved the field forward together through model improvement and mathematical analysis (WGAN [169]) modifications. The same attention has been focused on the application and research of GAN models in the IR image super-resolution.

Initially, GAN models using normal images have been directly used in IR image reconstruction. Researchers [170] used SRGAN straightly to reconstruct IR images and received reconstructed images that were quite acceptable. However, the blurred edges and unclear details are still a challenge. [121] used a modified DCGAN to reconstruct IR images, but the experimental results were not compared between the same category GAN methods. For this reason, it is difficult to describe the actual effectiveness. On the other hand, the work from [171] compared the existing SR algorithms cross-sectionally on IR images. The experimental results show that the SRFBN [172] model has the best universalization ability. But, for the GAN model, there are always unpleasant artifacts due to the model collapse. All these works illustrate the domain transfer difficulties possibly suffered by algorithms using visible images that are used in the IR images super-resolution task. Then, people started to consider the possibility of designing GAN models specifically for IR images. These studies are divided into the following categories: **module improvement, introduce extra information**.

1) *Module improvement*: It is natural first to consider that the improvement method is to explore new modules to improve performance. *Rivadeneira et al.* [173] uses the CycleGAN structure and employs ResNet as the generator's encoder. The self-attentive module is applied in the encoder and a new

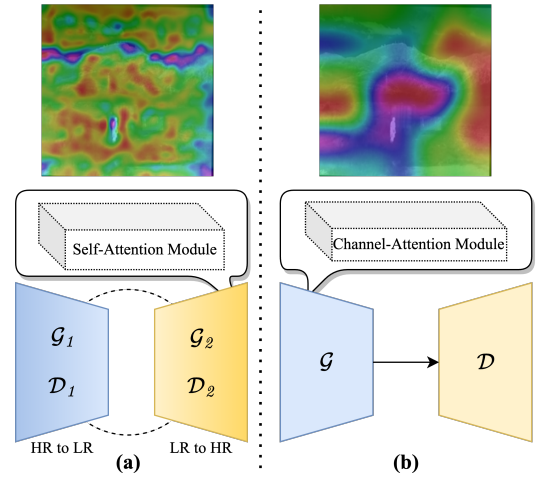


Fig. 10. Attentional mechanisms and GAN-based models for IR image super-resolution. Cam Heatmap is also presented.

loss function is also proposed (see Eq. 10). According to the discussion in this work, the Sobel edge detector can capture the contour consistency between the input image and the cyclic-generated image by calculating the mean squared difference between the images.

$$\mathcal{L}_{\text{Sobel}} = \frac{1}{N} \sum_i \|\text{Sobel}(G_{H2L}(G_{L2H}(I_L))) - \text{Sobel}(I_L)\| \quad (10)$$

Another GAN model based on the attention mechanism has also been proposed, which differs in the loss function and discriminator used [126]. As shown in Fig. 10. Liu, Qing-Ming, et al. use a module based on the channel attention mechanism in the generator at their work. Moreover, they also replaced the original discriminator with a new one designed by the gradient penalty approach from WGAN. It will benefit network convergence. For the loss function, Wasserstein distance is used to evaluate the target image I_{HR} and the reconstructed image \hat{I} (see Eq.11).

$$\mathcal{L}_{\text{WGAN}} = E[D_{\theta}(I_{HR}) - D_{\theta}(G_{\theta}(I_{LR}))] +, \quad (11)$$

$$\lambda E \left[\left\| \nabla_{I_D}(\hat{I})_2 - 1 \right\|^2 \right]$$

where the second term on the right side of the equal sign is the gradient penalty term. Furthermore, WGAN is used to optimize the training process is also mentioned in this work [159].

2) *Introduce extra information*: This approach is focused on the issue that IR images have fewer patterns and further proposes to use visible images to guide the reconstruction. The main options include the following: **hybrid and split**. For the hybrid model, the features from visible and IR images are not purposely distinguished but mixed directly in the module. In [18], the information is initially extracted by residual blocks and then fused using 1x1 convolution. It is called multimodal, visual-thermal fusion model. Experiments show that visible images are beneficial for improving high-frequency details in IR images.

For the split model, *Huang et al. [122]* proposed using transfer learning to help introduce the patterns in visible images to reconstruct IR images. In this approach, PSRGAN, two components are proposed: the main path, which is responsible for extracting the features from visible images, and the branch path, which is used to represent the patterns from IR images. Finally, the IR image is reconstructed by a transfer learning strategy that maps both of them to a common feature space. Such an approach can better capture and utilize the features in the model and show better results in the experiments.

Finally, there are also approaches that focus on the connection between SR methods and other tasks, such as denoising, and then models that combine cross-tasks are proposed. *Batchuluun, Ganbayar, et al. [174]* proposed methods that can be used for super-resolution and detection, where the super-resolution component focuses on both denoising and SR. In this work, the number of modules in the generator has been increased. In [175], researchers proposed a GAN-based framework for joint cross-modal and super-resolution aerial image vehicle detection. The first sub-network of this approach uses the GAN architecture to generate two different SR images by cross-domain transforms.

In summary, there is no doubt that the GAN model has great advantages in the field of generation, leading to a fairly good performance in SR algorithms. The results achieved in the visible field have attracted the application to the IR image super-resolution. However, according to the experimental results, the direct unmodified introduction of the normal image super-resolution reconstruction method encounters the difficulty of domain shift [121], [170], [171]. The edges in the reconstructed images are not clear. Therefore, new models have been proposed by considering the characteristics of IR images. These models are divided into improved modules [14], [126], [173], introduce extra information [18], [176], [177], and multitask [22], [129], [174], [175]. These algorithms have achieved some success, but missing standard benchmarks and datasets that are uniform leads to an unfavorable cross-sectional comparison between different types of methods. In the next section, we present available datasets and evaluation metrics in the IR image super-resolution field.

3) *Transformer-based*: Transformer-based methods have transformed IRSR by addressing challenges unique to IR imaging, such as low contrast and limited gradients. Leveraging self-attention mechanisms [180], these models excel in capturing long-range dependencies, making them ideal for reconstructing high-resolution IR images with superior structural consistency.

The architectural innovations within Transformer-based IR SR models demonstrate a strong focus on achieving efficient global feature representation. Swin Transformer-based models, such as SwinIBSR [30] and SwinIPISR [181], extend the Swin architecture with residual connections and tailored degradation models, improving generalization and robustness in real-world scenarios. Similarly, LKFormer replaces conventional self-attention with large kernel convolutional attention blocks, striking a balance between computational efficiency and non-local feature modeling [182]. These advancements reflect a shared objective to optimize performance while maintaining scalability.

A defining characteristic of these methods is their adaptability to specific tasks and modalities. Techniques like Cross-modal Texture Transformers (CMTT) effectively transfer information from visible-spectrum images to improve IR image quality, while edge-focused models such as TESR incorporate auxiliary networks to enhance texture and detail recovery [183]. Meanwhile, DASR utilizes dual-attention mechanisms to simultaneously capture local and global information, underscoring the versatility of Transformer architectures in addressing diverse challenges [184].

Compared to GANs, which excel in texture synthesis but are prone to artifacts under domain shifts, Transformer-based methods demonstrate superior robustness through explicit global contextual modeling. Similarly, while CNNs are computationally efficient and effective in learning localized features, Transformers outperform in scenarios requiring long-range dependency modeling and structural consistency. These distinctions make Transformers particularly suitable for dynamic environments where IR imaging data is sparse or noisy. For instance, TnTViT-G [29] demonstrates how visible-spectrum guidance can compensate for missing IR image details, exemplifying the potential of cross-spectral applications.

In summary, Transformer-based methods represent a significant advancement in IRSR by combining efficient feature extraction with innovative attention mechanisms. However, their computational complexity remains a challenge, particularly for high-resolution IR image reconstruction, where scaling attention mechanisms can be resource-intensive. Addressing these limitations could further enhance their applicability in real-time systems. These approaches share a unified goal of overcoming the limitations of IR imaging systems while optimizing for scalability and practical deployment. Future research will likely explore deeper integration with emerging imaging modalities and further enhancements for real-time applications.

IV. DATASETS & METRICS

We will present the datasets and image quality assessment metrics applied in the IR image super-resolution, respectively.

A. Datasets

For the super-resolution study, the datasets included: the training dataset and test dataset. Considering the training dataset, we hope that the samples are large enough to cover the current natural and realistic situations. It will be beneficial

TABLE VII

AVAILABLE DATASET IN IR IMAGE SUPER-RESOLUTION FIELDS. FROM LEFT TO RIGHT, THE COLUMNS DEPICT THE NAME AND THE REFERENCE, PIXEL RESOLUTION OF IMAGES, AND A BRIEF DESCRIPTION, RESPECTIVELY

Name	Classes	pxl	Description
NATO SET-140 [178]	Universal	320x256 640x480 384x288x2	The imagery was recorded for different target / background settings, camera and/or object movements and temperature contrasts. The paired samples are from the real world.
CASIA Interval v3 [146]	Iris images	280x320	This database has 2,655 NIR images of 280x320 pixels from 249 contributors captured in 2 sessions with a close-up iris camera, totaling 396 different eyes. HR-LR image pairs could be available from bicubic downsampling processing.
ULB17-VT [18]	Universal	240 x 320	Thermal and RGB images were manually extracted and annotated with a total of 570 pairs. The framework is divided into 512 training and validation samples and 58 test samples.
IR-COLOR2000 [179]	Universal	128x128	The training datasets (IR-COLOR2000), which contain 2000 pairs of images. Paired RGB images are available.
IR100 [122]	Universal	640x480	100 samples from FIR Sequence Pedestrian Dataset, the paired LR images come from bicubic downsampling.
CVC-09-1K [159]	Universal	640x480	1000 randomly selected images from the FIR Dataset, the paired LR images come from bicubic downsampling.
New dataset [130]	Universal	640x512	This dataset was acquired using a TAU2 thermal camera with a 13mm lens (45° HFOV) in a resolution of 640x512, with a depth of 8 bits and save it in PNG format
CDN-MRF dataset [132]	Universal	640x480	They build up a HR infrared image dataset covering a wide range of scenarios (e.g., vehicle, machine, pedestrian and building). The paired samples are from the real world.

to the models' generalization. For the test dataset, we would like to have standard datasets corresponding to different tasks. For example, in the face reconstruction task, the face dataset is important. But for iris reconstruction, the iris dataset would be more useful.

Datasets for IR images and video are available in other research topics [28], but fewer are focused on super-resolution. Despite the availability of datasets such as IR100 and NATO SET-140, current datasets often lack paired samples that span diverse environmental conditions or integrate multi-modal information. Future efforts should prioritize creating datasets reflecting real-world challenges, such as adverse weather conditions, varying lighting, and diverse environmental scenarios. Additionally, generative models offer a promising solution to data scarcity by synthesizing diverse training samples, and enhancing model robustness. We will present the following representative work: *Weiss et al. [178]* present a publicly distributable dataset for the assessment of fusion, super-resolution, local contrast enhancement, dynamic range compression, and performance of image-based non-uniformity correction (NUC) algorithms. This dataset records images for different target background settings, camera or object movements, and temperature contrasts. Furthermore, *Alonso-Fernandez et al.* present 1,872 NIR iris image datasets [185]. *Almasi & Debeir [66]*, on the other hand, presented a benchmark ULB17-VT dataset containing thermal images and their corresponding visual images. *Du, Juan, et al. [179]* also presented their dataset. For small sample reconstruction, *Huang, Yongsong, et al.* proposed the IR100 dataset [122]. *Huang, Yongsong, et al. [159]* further proposed a universal dataset including 1000 samples. The details are shown in Tab.VII. Although there exists plenty of work on IR image super-resolution, it is limited in releasing the dataset.

For the test dataset, it is very common to select a small sample from the training dataset. These images are used as reference samples to evaluate the algorithm performance. On

the other hand, IR image super-resolution is to be used in fused images sometimes. Considering this situation, there are also some algorithms [122], [159] that use fused images as reference, such as result-A [186] and result-C [187]. Different types of IR image samples will be useful to evaluate the reconstruction algorithm's robustness.

There are still some weaknesses in these datasets, which include the following aspects: these data are collected without indicating the relevant equipment parameters, which could influence the dataset selection in real situations. In addition, these datasets have different sample sizes. It is not conducive to compare them with each other. Furthermore, some datasets have no matching high-resolution visible image datasets, which causes difficulties in introducing the patterns from visible images. For datasets, we can make more efforts to complete the standard. On the other hand, it is also important to evaluate the reconstructed image quality. Then researchers also started to focus on proposing evaluation metrics applicable to infrared images which are also called IQA metrics.

B. Metrics

In the field of image reconstruction, how to evaluate reconstructed images is also a popular topic. We usually have three types of image evaluation metrics: **reference metrics**, **non-reference metrics**, and **human evaluation**.

1) *Reference metrics*: For reference metrics, the most commonly used to evaluate the algorithms' performance are peak signal-to-noise ratio (PSNR) and structural similarity index (SSIM). First, PSNR uses the maximum pixel value (denoted as L) and the mean square error (MSE) between images to estimate the reconstructed image quality. As shown in Eq. 12:

$$\text{PSNR} = 10 \cdot \log_{10} \left(\frac{L^2}{\frac{1}{N} \sum_{i=1}^N (I(i) - \hat{I}(i))^2} \right) \quad (12)$$

where L equals to 255 in general cases using 8-bit representations, I denotes the high resolution image while \hat{I} represents the reconstructed image. Since PSNR is only related to pixel-level MSE and only cares about the differences between corresponding pixels without concerns about visual perception, it tends to lead to poor performance in reconstruction quality in real scenes, while we are usually more concerned with human perception. But in order to compare with other work, we always need to calculate this metric. Then, the metric closer to the human subjective evaluation was proposed: SSIM [188].

SSIM is dedicated to measuring structural similarity between images, based on independent comparisons with brightness $\mathcal{C}_l(I, \hat{I})$, contrast $\mathcal{C}_c(I, \hat{I})$ and structural $\mathcal{C}_s(I, \hat{I})$ aspects (see Eq.13).

$$\text{SSIM}(I, \hat{I}) = \left[\mathcal{C}_l(I, \hat{I}) \right]^\alpha \left[\mathcal{C}_c(I, \hat{I}) \right]^\beta \left[\mathcal{C}_s(I, \hat{I}) \right]^\gamma \quad (13)$$

where α, β, γ are control parameters for adjusting the relative importance. More calculation details can be found in [188]. In short, SSIM evaluates the reconstruction quality from the perspective of human visual system [189]. Therefore, it better meets the requirements for perceptual evaluation [190], [191] and has been widely used in IR image super-resolution. In summary, the assessment of reference metrics always requires ground-truth images for comparison. In the real world, there is no ground-truth image. Then, no reference metrics are proposed.

2) *No reference metrics*: We will briefly describe the representative work of no reference metrics. The Natural Image Quality Evaluator (NIQE) [192] is a statistical collection of "quality-aware" features built on a simple but successful Natural Scene Statistics (NSS) model in the spatial domain. The researchers also evaluated the perceptual image patch similarity (LPIPS) directly through the trained deep network based on the difference in depth features. According to the experimental results, it would be fairer to use the features extracted by the CNN to evaluate the image quality [193].

3) *Human evaluation*: Human subjective evaluation is the best indicator. In general, we need to evaluate and then score the reconstructed images. However, in order to exclude errors due to visual fatigue, we need more participants and more time to remove biased data. In other words, the time and resource cost for this evaluation method would be the most expensive.

4) *Assessment of IR image super-resolution*: For IR images, which suffer from missing rich details and colors. It may be difficult to indicate the real image quality by directly using the usual visible image metrics as evaluation.

In [194], the researchers propose a non-reference metric: Q_{SR} . It is actually combined previous works [195] and this metric can be used not only to help the algorithm converge but also to evaluate the image quality. As shown in Eq. 14, where λ_1 and λ_2 are hyperparameters. According to the literature [194], this metric takes the balance between the no-reference and reference metrics into consideration and provides a better assessment on the image quality.

$$Q_{SR} = \lambda_1 \frac{1}{\log_{10}(S_{\text{BRISQUE}})} + \lambda_2 S_{\text{PSNR}} \quad (14)$$

V. FUTURE TRENDS

In this work, we systematically review the excellent previous work on IR image super-resolution and make a comparison with the summary. Thus, we will introduce some attractive directions in this field and ideas that will further improve the model performance in this section.

A. New models & new paradigms.

Good model design can improve the reconstructed image quality by better nonlinear mapping to represent complex patterns in high-dimensional space. As we embrace the advent of Large Language Models (LLMs) in the realm of natural language processing, it is also pertinent to consider the potential impact that the forthcoming Large Vision Models (LVMs) may have on the task of IR image super-resolution. For the new paradigm, we expect that the correlation between low and high frequency information in IR images will be studied to explain the correlation between them. We will present more details below.

Generative Models. With the rapid advancement of deep learning, state-space models and diffusion models [196]–[199] are gaining increasing attention in the community. State-space models, known for their efficient handling of long-range dependencies and scalability, offer a compelling alternative to traditional Transformer architectures for low-level vision tasks. We anticipate that the classical challenge of IR image super-resolution will significantly benefit from the integration of these state-of-the-art generative models.

Data Augmentation. A novel data augmentation approach for guided thermal image super-resolution generates synthetic thermal-like images from visible spectrum inputs using CycleGAN, effectively aligning the guiding and guided domains to enhance model performance [200]. Looking ahead, the development of advanced data augmentation paradigms, including domain-specific synthetic data generation and cross-modality transformations, represents a promising direction for overcoming data scarcity and improving model robustness in real-world applications.

Large Vision Models. Large Language Models have revolutionized the field of natural language processing, enabling machines to understand and generate human-like text. Drawing parallels, the development of Large Vision Models can have a profound impact on the field of computer vision, particularly in tasks like IR image super-resolution. IR image super-resolution faces challenges from intrinsic noise and low-resolution characteristics. LVMs, with their capacity to discern complex patterns and structures from vast data sets, can significantly bolster the efficacy of super-resolution tasks. They possess the ability to extract and upscale intricate details embedded within LR infrared images, thereby enhancing the quality and applicability of the resultant images. Furthermore, akin to LLMs, LVMs can utilize transfer learning to extrapolate the knowledge gleaned from extensive visual data sets to the task of IR super-resolution. This can mitigate the requirement for substantial amounts of infrared-specific training data, which is often challenging to procure.

B. New application

With the development in the field of image super-resolution, blind super-resolution is the future-oriented direction [201]–[204]. Although many models or algorithms have been proposed for image super-resolution, the performance in the real world is not ideal. The main problem is that these algorithms simply summarize the degradation as bicubic downsampling and ignore the blurred kernels that exist in the real world, such as noise and compression [9], [13], [205]–[207]. Thus, studies on real-world super-resolution of visible images began to attract the attention of researchers. In IR images, to make the algorithms applicable in the real world, we can pay more attention to the degradation models of IR imaging and design the corresponding reconstruction algorithms. All these works will help the algorithms to face the complex degradation environment.

C. Dataset and evaluation metrics

On the one hand, datasets, the cornerstone for algorithm training, are fundamental to this task. As mentioned before, there are many works on IR image super-resolution that have not released datasets, for various reasons. Considering this situation, we need to establish benchmarks for this task. A robust enough dataset will be needed, including optical device details, image sizes, and other capture information. It will be beneficial to compare the performance between different types of algorithms. If a matching dataset with visible images, captured under the same environmental conditions, could also be included, there is no doubt that it would help to validate the effectiveness of introducing visible image patterns. Moreover, available datasets are also provided for thermal infrared image challenges as well. For example, the Thermal Image Super-Resolution (TISR) challenge organized in the Perception Beyond the Visible Spectrum (PBVS) is one of the promising events. This challenge provides the training dataset and the test dataset with 951 and 50 samples, respectively [208], [209].

On the other hand, researchers also need reliable evaluation metrics to evaluate the algorithm's performance. We can design specialized evaluation metrics for IR images to determine the reconstructed image quality, whether it is a reference metric or a non-reference metric. Although infrared images have unique pattern information compared to visible images, it would be pioneering work if new evaluation metrics could be used in image evaluation cross-domain.

VI. CONCLUSION

In this paper, we provide a comprehensive survey of IR image super-resolution research from the past two decades. We discuss its fundamental role in engineering applications and analyze key factors limiting IR imaging quality, such as noise and hardware constraints, highlighting the high costs associated with hardware redesign. We systematically classify and summarize both traditional algorithms and deep learning-based methods, alongside essential datasets and image quality assessment metrics. Our review bridges the gap between traditional super-resolution approaches and the unique challenges

of IR imaging, offering actionable insights for developing domain-specific algorithms. Future research could explore integrating Large Vision Models and advanced data augmentation techniques to address current limitations and expand the applicability of IR image super-resolution in diverse real-world scenarios.

ACKNOWLEDGMENTS

This work was supported by JSPS KAKENHI Grant Number JP23KJ0118. All data included in this study are available upon request by contact with the corresponding author.

REFERENCES

- [1] Z. Wang, J. Chen, and S. C. Hoi, "Deep learning for image super-resolution: A survey," *IEEE transactions on pattern analysis and machine intelligence*, vol. 43, no. 10, pp. 3365–3387, 2020.
- [2] S. C. Park, M. K. Park, and M. G. Kang, "Super-resolution image reconstruction: a technical overview," *IEEE signal processing magazine*, vol. 20, no. 3, pp. 21–36, 2003.
- [3] H. Chen, X. He, L. Qing, Y. Wu, C. Ren, R. E. Sheriff, and C. Zhu, "Real-world single image super-resolution: A brief review," *Information Fusion*, vol. 79, pp. 124–145, 2022.
- [4] A. Liu, Y. Liu, J. Gu, Y. Qiao, and C. Dong, "Blind image super-resolution: A survey and beyond," *IEEE Transactions on Pattern Analysis and Machine Intelligence*, 2022.
- [5] J. Yang, J. Wright, T. Huang, and Y. Ma, "Image super-resolution as sparse representation of raw image patches," in *2008 IEEE conference on computer vision and pattern recognition*, pp. 1–8, IEEE, 2008.
- [6] J. Yang, J. Wright, T. S. Huang, and Y. Ma, "Image super-resolution via sparse representation," *IEEE transactions on image processing*, vol. 19, no. 11, pp. 2861–2873, 2010.
- [7] C. Dong, C. C. Loy, K. He, and X. Tang, "Image super-resolution using deep convolutional networks," *IEEE transactions on pattern analysis and machine intelligence*, vol. 38, no. 2, pp. 295–307, 2015.
- [8] C. Ledig, L. Theis, F. Huszár, J. Caballero, A. Cunningham, A. Acosta, A. Aitken, A. Tejani, J. Totz, Z. Wang, *et al.*, "Photo-realistic single image super-resolution using a generative adversarial network," in *Proceedings of the IEEE conference on computer vision and pattern recognition*, pp. 4681–4690, 2017.
- [9] X. Wang, L. Xie, C. Dong, and Y. Shan, "Real-esrgan: Training real-world blind super-resolution with pure synthetic data," in *Proceedings of the IEEE/CVF International Conference on Computer Vision*, pp. 1905–1914, 2021.
- [10] J. Liang, J. Cao, G. Sun, K. Zhang, L. Van Gool, and R. Timofte, "Swinir: Image restoration using swin transformer," in *Proceedings of the IEEE/CVF International Conference on Computer Vision*, pp. 1833–1844, 2021.
- [11] Z. Gao and J. Chen, "Maritime infrared image super-resolution using cascaded residual network and novel evaluation metric," *IEEE Access*, vol. 10, pp. 17760–17767, 2022.
- [12] Z. Luo, Y. Huang, S. Li, L. Wang, and T. Tan, "Learning the degradation distribution for blind image super-resolution," in *Proceedings of the IEEE/CVF Conference on Computer Vision and Pattern Recognition*, pp. 6063–6072, 2022.
- [13] K. Zhang, J. Liang, L. Van Gool, and R. Timofte, "Designing a practical degradation model for deep blind image super-resolution," in *Proceedings of the IEEE/CVF International Conference on Computer Vision*, pp. 4791–4800, 2021.
- [14] K. Prajapati, V. Chudasama, H. Patel, A. Sarvaiya, K. P. Upla, K. Raja, R. Ramachandra, and C. Busch, "Channel split convolutional neural network (chasnet) for thermal image super-resolution," in *Proceedings of the IEEE/CVF Conference on Computer Vision and Pattern Recognition*, pp. 4368–4377, 2021.
- [15] Y. Wang, J. Zhang, and L. Wang, "Compressed sensing super-resolution method for improving the accuracy of infrared diagnosis of power equipment," *Applied Sciences*, vol. 12, no. 8, p. 4046, 2022.
- [16] B. Wang, Y. Zou, L. Zhang, L. Li, and C. Zuo, "Super resolution reconstruction of low light level image based on the feature extraction convolution neural network," in *Computational Imaging VI*, vol. 11731, pp. 74–79, SPIE, 2021.

- [17] Y. Yang, Q. Li, C. Yang, Y. Fu, H. Feng, Z. Xu, and Y. Chen, "Deep networks with detail enhancement for infrared image super-resolution," *IEEE Access*, vol. 8, pp. 158690–158701, 2020.
- [18] F. Almasri and O. Debeir, "Multimodal sensor fusion in single thermal image super-resolution," in *Asian Conference on Computer Vision*, pp. 418–433, Springer, 2018.
- [19] G. Suryanarayana, E. Tu, and J. Yang, "Infrared super-resolution imaging using multi-scale saliency and deep wavelet residuals," *Infrared Physics & Technology*, vol. 97, pp. 177–186, 2019.
- [20] A. Güngör and O. F. Kar, "A transform learning based deconvolution technique with super-resolution and microscanning applications," in *2019 IEEE International Conference on Image Processing (ICIP)*, pp. 2159–2163, IEEE, 2019.
- [21] X. Zhang, W. Huang, M. Xu, S. Jia, X. Xu, F. Li, and Y. Zheng, "Super-resolution imaging for infrared micro-scanning optical system," *Optics express*, vol. 27, no. 5, pp. 7719–7737, 2019.
- [22] X. Liu, Y. Chen, Z. Peng, and J. Wu, "Infrared image super-resolution reconstruction based on quaternion and high-order overlapping group sparse total variation," *Sensors*, vol. 19, no. 23, p. 5139, 2019.
- [23] X. Zhang, C. Li, Q. Meng, S. Liu, Y. Zhang, and J. Wang, "Infrared image super resolution by combining compressive sensing and deep learning," *Sensors*, vol. 18, no. 8, p. 2587, 2018.
- [24] Z. Gang, Z. Kai, S. Wei, and Y. Jie, "A study on nsct based super-resolution reconstruction for infrared image," in *2013 IEEE International Conference of IEEE Region 10 (TENCON 2013)*, pp. 1–5, IEEE, 2013.
- [25] T. Y. Han, D. H. Kim, S. H. Lee, and B. C. Song, "Infrared image super-resolution using auxiliary convolutional neural network and visible image under low-light conditions," *Journal of Visual Communication and Image Representation*, vol. 51, pp. 191–200, 2018.
- [26] I. Marivani, E. Tsilianni, B. Cornelis, and N. Deligiannis, "Multimodal deep unfolding for guided image super-resolution," *IEEE Transactions on Image Processing*, vol. 29, pp. 8443–8456, 2020.
- [27] L. Wang and K.-J. Yoon, "Deep learning for hdr imaging: State-of-the-art and future trends," *IEEE Transactions on Pattern Analysis and Machine Intelligence*, 2021.
- [28] K. I. Danaci and E. Akagunduz, "A survey on infrared image and video sets," *arXiv preprint arXiv:2203.08581*, 2022.
- [29] A. Mehri, P. Behjati, and A. D. Sappa, "Tntvit-g: Transformer in transformer network for guidance super resolution," *IEEE Access*, vol. 11, pp. 11529–11540, 2023.
- [30] Y. Shi, N. Chen, Y. Pu, J. Zhang, and L. Yao, "Swinibr: Towards real-world infrared image super-resolution," *Infrared Physics & Technology*, vol. 139, p. 105279, 2024.
- [31] Y. Zhang, P. Zhou, and L. Chen, "Dual-branch feature encoding framework for infrared images super-resolution reconstruction," *Scientific Reports*, vol. 14, no. 1, p. 9379, 2024.
- [32] J. Han, X. Chen, L. Feng, L. Yang, and T. Qin, "Dual discriminators generative adversarial networks for unsupervised infrared super-resolution," *Infrared Physics & Technology*, vol. 133, p. 104836, 2023.
- [33] Y. Huang, T. Miyazaki, X. Liu, and S. Omachi, "Irsrmamba: Infrared image super-resolution via mamba-based wavelet transform feature modulation model," *arXiv preprint arXiv:2405.09873*, 2024.
- [34] M. Läikin, *Lens design*. CRC Press, 2018.
- [35] H. Yuan, F. Yan, X. Chen, and J. Zhu, "Compressive hyperspectral imaging and super-resolution," in *2018 IEEE 3rd International Conference on Image, Vision and Computing (ICIVC)*, pp. 618–623, IEEE, 2018.
- [36] H. J. Rabal and R. A. Braga Jr, *Dynamic laser speckle and applications*. CRC press, 2018.
- [37] H. Lee, T. Olson, D. Manville, and G. Cloud, "Image analysis and understanding using super resolution," in *Display Technologies and Applications for Defense, Security, and Avionics*, vol. 6558, pp. 95–101, SPIE, 2007.
- [38] A. Mas, G. Druart, and F. De La Barrière, "Study of asymmetric or decentered multi-view designs for uncooled infrared imaging applications," *Optics Express*, vol. 28, no. 23, pp. 35216–35230, 2020.
- [39] P. Bijl, J. A. Beintema, N. van der Leden, and J. Dijk, "Effectiveness assessment of signal processing in the presence of smear," *Optical Engineering*, vol. 51, no. 6, p. 063205, 2012.
- [40] S.-H. Kim, B.-S. Choi, J. Lee, J. Lee, J.-H. Park, K.-I. Lee, and J.-K. Shin, "Averaging current adjustment technique for reducing pixel resistance variation in a bolometer-type uncooled infrared image sensor," *Journal of Sensor Science and Technology*, vol. 27, no. 6, pp. 357–361, 2018.
- [41] S.-P. Wang, "Stripe noise removal for infrared image by minimizing difference between columns," *Infrared Physics & Technology*, vol. 77, pp. 58–64, 2016.
- [42] L. Chen, Z. Zhou, N. Xi, R. Yang, B. Song, Z. Sun, and C. Su, "Super resolution infrared camera using single carbon nanotube photodetector," in *SENSORS, 2014 IEEE*, pp. 1038–1041, IEEE, 2014.
- [43] W. Kong, P. Cao, X. Zhang, L. Cheng, T. Wang, L. Yang, and Q. Meng, "Near-infrared super resolution imaging with metallic nanoshell particle chain array," *Plasmonics*, vol. 8, no. 2, pp. 835–842, 2013.
- [44] K. Schutte, D.-J. J. de Lange, and S. P. van den Broek, "Signal conditioning algorithms for enhanced tactical sensor imagery," in *Infrared Imaging Systems: Design, Analysis, Modeling, and Testing XIV*, vol. 5076, pp. 92–100, SPIE, 2003.
- [45] S. Ming-Jie, Y. Kang-long, and X. Zhi, "Effect of pixel active area shapes in microscanning based infrared super-resolution imaging," in *2013 Third International Conference on Instrumentation, Measurement, Computer, Communication and Control*, pp. 909–912, IEEE, 2013.
- [46] M. Sun and K. Yu, "A sur-pixel scan method for super-resolution reconstruction," *Optik*, vol. 124, no. 24, pp. 6905–6909, 2013.
- [47] N. Kopeika, A. Abramovich, A. Levanon, A. Akram, D. Rozban, Y. Yitzhaky, O. Yadid-Pecht, and A. Belenky, "Sub-wavelength resolution of mmw imaging systems using extremely inexpensive scanning glow discharge detector (gdd) double row camera," in *Passive and Active Millimeter-Wave Imaging XV*, vol. 8362, pp. 127–134, SPIE, 2012.
- [48] S. S. Young and R. G. Driggers, "Superresolution image reconstruction from a sequence of aliased imagery," *Applied Optics*, vol. 45, no. 21, pp. 5073–5085, 2006.
- [49] W. Yu, Q. Peng, H. Tu, and Z. Wang, "An infrared image synthesis model based on infrared physics and heat transfer," *International journal of infrared and millimeter waves*, vol. 19, pp. 1661–1669, 1998.
- [50] C. Oh, N. Nandhakumar, and J. K. Aggarwal, "Integrated modelling of thermal and visual image generation," in *1989 IEEE Computer Society Conference on Computer Vision and Pattern Recognition*, pp. 356–357, IEEE Computer Society, 1989.
- [51] N. Nandhakumar, S. Karthik, and J. K. Aggarwal, "Unified modeling of non-homogeneous 3d objects for thermal and visual image synthesis," *Pattern recognition*, vol. 27, no. 10, pp. 1303–1316, 1994.
- [52] H.-K. Hong, S.-H. Han, G.-P. Hong, and J.-S. Choi, "Simulation of reticle seekers using the generated thermal images," in *Proceedings of APCCAS'96-Asia Pacific Conference on Circuits and Systems*, pp. 183–186, IEEE, 1996.
- [53] M. Offroy, Y. Roggo, and L. Duponchel, "Increasing the spatial resolution of near infrared chemical images (nir-ci): The super-resolution paradigm applied to pharmaceutical products," *Chemometrics and Intelligent Laboratory Systems*, vol. 117, pp. 183–188, 2012.
- [54] M. Offroy, Y. Roggo, P. Milanfar, and L. Duponchel, "Infrared chemical imaging: spatial resolution evaluation and super-resolution concept," *Analytica chimica acta*, vol. 674 2, pp. 220–6, 2010.
- [55] I. H. Lee, W.-Y. Chung, and C.-G. Park, "Super-resolution thermal generative adversarial networks for infrared image enhancement," *Journal of Institute of Control, Robotics and Systems*, 2022.
- [56] H. Gupta and K. Mitra, "Toward unaligned guided thermal super-resolution," *IEEE Transactions on Image Processing*, vol. 31, pp. 433–445, 2022.
- [57] J. Shen, K. Wang, K. Yang, K. Xiang, L. Fei, X. Hu, H. Li, and H. Chen, "A depth estimation framework based on unsupervised learning and cross-modal translation," in *Target and Background Signatures V*, vol. 11158, pp. 21–31, SPIE, 2019.
- [58] T. Rukkanchanunt, M. Tanaka, and M. Okutomi, "Image enhancement framework for low-resolution thermal images in visible and lwir camera systems," in *Emerging Imaging and Sensing Technologies for Security and Defence II*, vol. 10438, pp. 37–46, SPIE, 2017.
- [59] D. M. Martínez Gila, J. P. Navarro Soto, S. Satorres Martínez, J. Gómez Ortega, and J. Gámez García, "The advantage of multispectral images in fruit quality control for extra virgin olive oil production," *Food Analytical Methods*, vol. 15, no. 1, pp. 75–84, 2022.
- [60] H. Wang, R. Hu, M. Zhang, Z. Zhai, and R. Zhang, "Identification of tomatoes with early decay using visible and near infrared hyperspectral imaging and image-spectrum merging technique," *Journal of Food Process Engineering*, vol. 44, no. 4, p. e13654, 2021.
- [61] J. Torra, F. Viela, D. Megías, B. Sot, and C. Flors, "Versatile near-infrared super-resolution imaging of amyloid fibrils with the fluorogenic probe cranad-2," *Chemistry*, 2022.

- [62] M. R. Canales-Fiscal, R. O. López, R. Barzilay, V. Treviño, S. Cardona-Huerta, L. J. Ramírez-Treviño, A. Yala, and J. G. Tamez-Peña, "Covid-19 classification using thermal images: thermal images capability for identifying covid-19 using traditional machine learning classifiers," *Proceedings of the 12th ACM Conference on Bioinformatics, Computational Biology, and Health Informatics*, 2021.
- [63] J. Lukose, S. Chidangil, and S. D. George, "Optical technologies for the detection of viruses like covid-19: Progress and prospects," *Biosensors & Bioelectronics*, vol. 178, pp. 113004 – 113004, 2021.
- [64] H. Liu, Q. An, T. Liu, Z. Huang, and Q. Deng, "An infrared image denoising model with unidirectional gradient and sparsity constraint on biomedical images," *Infrared Physics & Technology*, vol. 126, p. 104348, 2022.
- [65] C. Bodensteiner, S. Bullinger, and M. Arens, "Multispectral matching using conditional generative appearance modeling," *2018 15th IEEE International Conference on Advanced Video and Signal Based Surveillance (AVSS)*, pp. 1–6, 2018.
- [66] F. Almasri and O. Debeir, "Multimodal sensor fusion in single thermal image super-resolution," in *ACCV Workshops*, 2018.
- [67] Q. Xiong, L. Di, Q. Feng, D. Liu, W. Liu, X. Zan, L. Zhang, D. Zhu, Z. Liu, X. Yao, *et al.*, "Deriving non-cloud contaminated sentinel-2 images with rgb and near-infrared bands from sentinel-1 images based on a conditional generative adversarial network," *Remote Sensing*, vol. 13, no. 8, p. 1512, 2021.
- [68] J. Nie, H. Ren, Y. Zheng, D. Ghent, and K. Tansey, "Land surface temperature and emissivity retrieval from nighttime middle-infrared and thermal-infrared sentinel-3 images," *IEEE Geoscience and Remote Sensing Letters*, vol. 18, no. 5, pp. 915–919, 2020.
- [69] C.-H. Lin and T.-Y. Wang, "A novel convolutional neural network architecture of multispectral remote sensing images for automatic material classification," *Signal Processing: Image Communication*, vol. 97, p. 116329, 2021.
- [70] M. L. M. Yaacob, A. S. A. Rashid, A. Ismail, R. Sa'ari, M. Mustaffar, N. M. Yusof, N. Abd Rahaman, *et al.*, "Rock slope monitoring using drone based multispectral and thermal images," in *IOP Conference Series: Earth and Environmental Science*, vol. 540, p. 012024, IOP Publishing, 2020.
- [71] C. Granero-Belinchon, A. Michel, V. Achard, and X. Briottet, "Spectral unmixing for thermal infrared multi-spectral airborne imagery over urban environments: day and night synergy," *Remote Sensing*, vol. 12, no. 11, p. 1871, 2020.
- [72] Y. Cao, G. L. Li, Y. K. Luo, Q. Pan, and S. Y. Zhang, "Monitoring of sugar beet growth indicators using wide-dynamic-range vegetation index (wdvri) derived from uav multispectral images," *Computers and Electronics in Agriculture*, vol. 171, p. 105331, 2020.
- [73] S. Liu, W. Zeng, L. Wu, G. Lei, H. Chen, T. Gaiser, and A. K. Srivastava, "Simulating the leaf area index of rice from multispectral images," *Remote Sensing*, vol. 13, no. 18, p. 3663, 2021.
- [74] H. Qi, B. Zhu, Z. Wu, Y. Liang, J. Li, L. Wang, T. Chen, Y. Lan, and L. Zhang, "Estimation of peanut leaf area index from unmanned aerial vehicle multispectral images," *Sensors*, vol. 20, no. 23, p. 6732, 2020.
- [75] R. Barzin, H. Kamangir, and G. C. Bora, "Comparison of machine learning methods for leaf nitrogen estimation in corn using multispectral uav images," *Transactions of the ASABE*, vol. 64, no. 6, pp. 2089–2101, 2021.
- [76] P. Yao-qi, X. Ying-xin, F. Ze-tian, D. Yu-hong, L. Xin-xing, Y. Hai-jun, and Z. Yong-jun, "Water content detection of maize leaves based on multispectral images," *Spectroscopy and Spectral Analysis*, vol. 40, no. 4, pp. 1257–1262, 2020.
- [77] D. Wen, A. Ren, T. Ji, I. M. Flores-Parra, X. Yang, and M. Li, "Segmentation of thermal infrared images of cucumber leaves using k-means clustering for estimating leaf wetness duration," *International Journal of Agricultural and Biological Engineering*, vol. 13, no. 3, pp. 161–167, 2020.
- [78] M. Kerkech, A. Hafiane, and R. Canals, "Vine disease detection in uav multispectral images using optimized image registration and deep learning segmentation approach," *Computers and Electronics in Agriculture*, vol. 174, p. 105446, 2020.
- [79] S. Wang, M. Ding, B. Xue, Y. Hou, and Y. Sun, "Live cell visualization of multiple protein-protein interactions with bifc rainbow," *ACS chemical biology*, vol. 13 5, pp. 1180–1188, 2018.
- [80] M. Beenard, D. Schapman, *et al.*, "Optimization of advanced live-cell imaging through red/near-infrared dye labeling and fluorescence lifetime-based strategies," *International Journal of Molecular Sciences*, vol. 22, 2021.
- [81] P. Dufour, S. Dufour, A. Castonguay, N. McCarthy, and Y. De Koninck, "Two-photon laser scanning fluorescence microscopy for functional cellular imaging: Advantages and challenges or one photon is good... but two is better!," *Medecine Sciences: M/S*, vol. 22, no. 10, pp. 837–844, 2006.
- [82] X. Zhou, L. Jiang, C. Hu, S. Lei, T. Zhang, and X. Mou, "Yolo-sase: An improved yolo algorithm for the small targets detection in complex backgrounds," *Sensors*, vol. 22, no. 12, p. 4600, 2022.
- [83] X. Li, S. Wang, B. Liu, W. Chen, W. Fan, and Z. Tian, "Improved yolov4 network using infrared images for personnel detection in coal mines," *Journal of Electronic Imaging*, vol. 31, pp. 013017 – 013017, 2022.
- [84] G. G. J. Ramos, J. C. S. Garcia, and V. Ponomariov, "Embedded system for real-time person detecting in infrared images/videos using super-resolution and haar-like feature techniques," in *2015 12th International Conference on Electrical Engineering, Computing Science and Automatic Control (CCE)*, pp. 1–6, IEEE, 2015.
- [85] D. T. Lloyd, A. Abela, R. A. Farrugia, A. Galea, and G. Valentino, "Optically enhanced super-resolution of sea surface temperature using deep learning," *IEEE Transactions on Geoscience and Remote Sensing*, vol. 60, pp. 1–14, 2021.
- [86] B. Ping, Y. Meng, C. Xue, and F. Su, "Can the structure similarity of training patches affect the sea surface temperature deep learning super-resolution?," *Remote Sensing*, vol. 13, no. 18, p. 3568, 2021.
- [87] X. Yang, Y. Li, Y. Wei, Z. Chen, and P. Xie, "Water body extraction from sentinel-3 image with multiscale spatiotemporal super-resolution mapping," *Water*, vol. 12, no. 9, p. 2605, 2020.
- [88] J. Lukose, S. Chidangil, and S. D. George, "Optical technologies for the detection of viruses like covid-19: Progress and prospects," *Biosensors & Bioelectronics*, vol. 178, p. 113004, 2021.
- [89] L. Mazaheri, J. Jelken, M. O. Avilés, S. Legge, and F. Lagugné-Labarthe, "Investigating the performances of wide-field raman microscopy with stochastic optical reconstruction post-processing," *Applied spectroscopy*, vol. 76, no. 3, pp. 340–351, 2022.
- [90] S. Zhang, K. Kniazev, I. M. Pavlovets, S. Zhang, R. L. Stevenson, and M. Kuno, "Deep image restoration for infrared photothermal heterodyne imaging," *The Journal of Chemical Physics*, vol. 155, no. 21, p. 214202, 2021.
- [91] I. M. Pavlovets, E. A. Podshivyaylov, P. A. Frantsuzov, G. V. Hartland, and M. Kuno, "Quantitative infrared photothermal microscopy," in *Single Molecule Spectroscopy and Superresolution Imaging XIII*, vol. 11246, pp. 126–132, SPIE, 2020.
- [92] Z. Li, M. Kuno, and G. Hartland, "Super-resolution imaging with mid-ir photothermal microscopy on the single particle level," in *Physical Chemistry of Interfaces and Nanomaterials XIV*, vol. 9549, pp. 121–128, SPIE, 2015.
- [93] M. Szankin, A. Kwasniewska, and J. Ruminski, "Influence of thermal imagery resolution on accuracy of deep learning based face recognition," in *2019 12th International Conference on Human System Interaction (HSI)*, pp. 1–6, IEEE, 2019.
- [94] M. Shao, Y. Wang, and Y. Wang, "A super-resolution based method to synthesize visual images from near infrared," in *2009 16th IEEE International Conference on Image Processing (ICIP)*, pp. 2453–2456, IEEE, 2009.
- [95] Z. Zhang, Y. Wang, and Z. Zhang, "Face synthesis from low-resolution near-infrared to high-resolution visual light spectrum based on tensor analysis," *Neurocomputing*, vol. 140, pp. 146–154, 2014.
- [96] X. Zhang, J. Yang, N. Liu, and J. Liu, "Edge multidirectional binary pattern applies to high resolution thermal infrared face database," in *Chinese Conference on Biometric Recognition*, pp. 508–515, Springer, 2015.
- [97] R. Redlich, L. Aranedra, A. Saavedra, and M. Figueroa, "An embedded hardware architecture for real-time super-resolution in infrared cameras," in *2016 Euromicro conference on digital system design (DSD)*, pp. 184–191, IEEE, 2016.
- [98] S. Chen, H. Ren, X. Ye, J. Dong, and Y. Zheng, "Geometry and adjacency effects in urban land surface temperature retrieval from high-spatial-resolution thermal infrared images," *Remote Sensing of Environment*, vol. 262, p. 112518, 2021.
- [99] B. Allred, L. Martinez, M. K. Fessehazion, G. Rouse, T. Koganti, R. Freeland, N. Eash, D. Wishart, and R. Featheringill, "Time of day impact on mapping agricultural subsurface drainage systems with uav thermal infrared imagery," *Agricultural Water Management*, vol. 256, p. 107071, 2021.
- [100] M. Yamaguchi, K. Akiyama, T. Tsukagoshi, T. Muto, A. Kataoka, F. Tazaki, S. Ikeda, M. Fukagawa, M. Honma, and R. Kawabe, "Super-resolution imaging of the protoplanetary disk hd 142527 using sparse modeling," *The Astrophysical Journal*, vol. 895, no. 2, p. 84, 2020.

- [101] P. M. Harvey, J. D. Adams, T. L. Herter, G. Gull, J. Schoenwald, L. D. Keller, J. M. De Buizer, W. Vacca, W. Reach, and E. Becklin, "First science results from sofia/forcast: Super-resolution imaging of the s140 cluster at 37 μm ," *The Astrophysical Journal Letters*, vol. 749, no. 2, p. L20, 2012.
- [102] B. Biller, L. Close, A. Li, J. Biegging, W. Hoffmann, P. Hinz, D. Miller, G. Brusa, M. Lloyd-Hart, F. Wildi, *et al.*, "High-resolution mid-infrared imaging of the asymptotic giant branch star rv bootis with the steward observatory adaptive optics system," *The Astrophysical Journal*, vol. 620, no. 1, p. 450, 2005.
- [103] S. Megeath, P. Cox, L. Bronfman, and P. Roelfsema, "Evidence for ongoing star formation in the carina nebula," *Astronomy and Astrophysics*, vol. 305, p. 296, 1996.
- [104] A. Morozumi, M. Kamiya, S.-N. Uno, K. Umezawa, R. Kojima, T. Yoshihara, S. Tobita, and Y. Urano, "Spontaneously blinking fluorophores based on nucleophilic addition/dissociation of intracellular glutathione for live-cell super-resolution imaging," *Journal of the American Chemical Society*, 2020.
- [105] S. F. H. Barnett, A. Hitchcock, A. K. Mandal, C. Vasilev, J. M. Yuen, J. Morby, A. A. Brindley, D. M. Niedzwiedzki, D. A. Bryant, A. J. Cadby, D. Holten, and C. N. Hunter, "Repurposing a photosynthetic antenna protein as a super-resolution microscopy label," *Scientific Reports*, vol. 7, 2017.
- [106] D. Baddeley, D. J. Crossman, S. Rossberger, J. E. Cheyney, J. M. Montgomery, I. D. Jayasinghe, C. Cremer, M. B. Cannell, and C. Soeller, "4d super-resolution microscopy with conventional fluorophores and single wavelength excitation in optically thick cells and tissues," *PLoS ONE*, vol. 6, 2011.
- [107] M. T. Proetto, C. E. Callmann, J. B. Cliff, C. Szymanski, D. Hu, S. B. Howell, J. E. Evans, G. Orr, and N. C. Gianneschi, "Tumor retention of enzyme-responsive pt(ii) drug-loaded nanoparticles imaged by nanoscale secondary ion mass spectrometry and fluorescence microscopy," *ACS Central Science*, vol. 4, pp. 1477 – 1484, 2018.
- [108] X. Zhou, L. Jiang, C. Hu, S. Lei, T. Zhang, and X. Mou, "Yolo-sase: An improved yolo algorithm for the small targets detection in complex backgrounds," *Sensors (Basel, Switzerland)*, vol. 22, 2022.
- [109] G. Ramos, J. C. García, and V. Ponomarev, "Embedded system for real-time person detecting in infrared images/videos using super-resolution and haar-like feature techniques," *2015 12th International Conference on Electrical Engineering, Computing Science and Automatic Control (CCE)*, pp. 1–6, 2015.
- [110] J. Shen, K. Wang, K. Xiang, K. Xiang, L. Fei, X. Hu, H. Li, and H. Chen, "A depth estimation framework based on unsupervised learning and cross-modal translation," in *Security + Defence*, 2019.
- [111] T. Rukkanchanunt, M. Tanaka, and M. Okutomi, "Image enhancement framework for low-resolution thermal images in visible and lwir camera systems," in *Security + Defence*, 2017.
- [112] M. Yamaguchi, K. Akiyama, T. Tsukagoshi, T. Muto, A. Kataoka, F. Tazaki, S. Ikeda, M. Fukagawa, M. Honma, and R. Kawabe, "Super-resolution imaging of the protoplanetary disk hd 142527 using sparse modeling," *The Astrophysical Journal*, vol. 895, 2020.
- [113] B. A. Biller, L. M. Close, A. Li, J. H. Biegging, W. F. Hoffmann, P. M. Hinz, D. T. Miller, G. Brusa, M. Lloyd-Hart, F. Wildi, D. E. Potter, and B. D. Oppenheimer, "High-resolution mid-infrared imaging of the asymptotic giant branch star rv bootis with the steward observatory adaptive optics system," *The Astrophysical Journal*, vol. 620, pp. 450 – 458, 2005.
- [114] S. T. Megeath, P. Cox, L. Bronfman, and P. R. Roelfsema, "Evidence for ongoing star formation in the carina nebula," *Astronomy and Astrophysics*, vol. 305, pp. 296–307, 1996.
- [115] P. Song, X. Deng, J. F. Mota, N. Deligiannis, P. L. Dragotti, and M. R. Rodrigues, "Multimodal image super-resolution via joint sparse representations induced by coupled dictionaries," *IEEE Transactions on Computational Imaging*, vol. 6, pp. 57–72, 2019.
- [116] M. Kim and Y. Kim, "Forward looking infrared images' resolution improvement applying an image restoration method of a super resolution," in *2009 34th International Conference on Infrared, Millimeter, and Terahertz Waves*, pp. 1–2, IEEE, 2009.
- [117] G. Sun, Q. Li, and L. Lu, "Map algorithm to super-resolution of infrared images," in *MIPPR 2007: Multispectral Image Processing*, vol. 6787, pp. 148–156, SPIE, 2007.
- [118] H.-c. Liu, S.-t. Li, and H.-t. Yin, "Infrared surveillance image super resolution via group sparse representation," *Optics Communications*, vol. 289, pp. 45–52, 2013.
- [119] X. Kuang, X. Sui, Y. Liu, Q. Chen, and G. Guohua, "Single infrared image optical noise removal using a deep convolutional neural network," *IEEE photonics Journal*, vol. 10, no. 2, pp. 1–15, 2017.
- [120] J. Zhong, B. Yang, Y. Li, F. Zhong, and Z. Chen, "Image fusion and super-resolution with convolutional neural network," in *Chinese Conference on Pattern Recognition*, pp. 78–88, Springer, 2016.
- [121] A.-C. Guei and M. Akhoulfi, "Deep learning enhancement of infrared face images using generative adversarial networks," *Applied optics*, vol. 57, no. 18, pp. D98–D107, 2018.
- [122] Y. Huang, Z. Jiang, R. Lan, S. Zhang, and K. Pi, "Infrared image super-resolution via transfer learning and psrgan," *IEEE Signal Processing Letters*, vol. 28, pp. 982–986, 2021.
- [123] H. Wu, X. Hao, J. Wu, H. Xiao, C. He, and S. Yin, "Deep learning-based image super-resolution restoration for mobile infrared imaging system," *Infrared Physics & Technology*, vol. 132, p. 104762, 2023.
- [124] E. Agustsson and R. Timofte, "Ntire 2017 challenge on single image super-resolution: Dataset and study," in *Proceedings of the IEEE conference on computer vision and pattern recognition workshops*, pp. 126–135, 2017.
- [125] W. Wu, T. Wang, Z. Wang, L. Cheng, and H. Wu, "Meta transfer learning-based super-resolution infrared imaging," *Digital Signal Processing*, vol. 131, p. 103730, 2022.
- [126] Q.-M. Liu, R.-S. Jia, Y.-B. Liu, H.-B. Sun, J.-Z. Yu, and H.-M. Sun, "Infrared image super-resolution reconstruction by using generative adversarial network with an attention mechanism," *Applied Intelligence*, vol. 51, no. 4, pp. 2018–2030, 2021.
- [127] I. Marivani, E. Tsiligianni, B. Cornelis, and N. Deligiannis, "Joint image super-resolution via recurrent convolutional neural networks with coupled sparse priors," in *2020 IEEE International Conference on Image Processing (ICIP)*, pp. 868–872, IEEE, 2020.
- [128] T. Yao, Y. Luo, J. Hu, H. Xie, and Q. Hu, "Infrared image super-resolution via discriminative dictionary and deep residual network," *Infrared Physics & Technology*, vol. 107, p. 103314, 2020.
- [129] G. Batchuluun, Y. W. Lee, D. T. Nguyen, T. D. Pham, and K. R. Park, "Thermal image reconstruction using deep learning," *IEEE Access*, vol. 8, pp. 126839–126858, 2020.
- [130] R. E. Rivadeneira, P. L. Suárez, A. D. Sappa, and B. X. Vintimilla, "Thermal image superresolution through deep convolutional neural network," in *International conference on image analysis and recognition*, pp. 417–426, Springer, 2019.
- [131] I. Marivani, E. Tsiligianni, B. Cornelis, and N. Deligiannis, "Multimodal image super-resolution via deep unfolding with side information," in *2019 27th European Signal Processing Conference (EU-SIPCO)*, pp. 1–5, IEEE, 2019.
- [132] Z. He, S. Tang, J. Yang, Y. Cao, M. Y. Yang, and Y. Cao, "Cascaded deep networks with multiple receptive fields for infrared image super-resolution," *IEEE transactions on circuits and systems for video technology*, vol. 29, no. 8, pp. 2310–2322, 2018.
- [133] C. Sun, J. Lv, J. Li, and R. Qiu, "A rapid and accurate infrared image super-resolution method based on zoom mechanism," *Infrared Physics & Technology*, vol. 88, pp. 228–238, 2018.
- [134] Y. Zhao, X. Sui, Q. Chen, and S. Wu, "Learning-based compressed sensing for infrared image super resolution," *Infrared Physics & Technology*, vol. 76, pp. 139–147, 2016.
- [135] J. Wang, J. F. Ralph, and J. Y. Goulermas, "An analysis of a robust super resolution algorithm for infrared imaging," in *2009 Proceedings of 6th International Symposium on Image and Signal Processing and Analysis*, pp. 158–163, IEEE, 2009.
- [136] K. Choi, C. Kim, M.-H. Kang, and J. B. Ra, "Resolution improvement of infrared images using visible image information," *IEEE signal processing letters*, vol. 18, no. 10, pp. 611–614, 2011.
- [137] Y. Mao, Y. Wang, J. Zhou, and H. Jia, "An infrared image super-resolution reconstruction method based on compressive sensing," *Infrared Physics & Technology*, vol. 76, pp. 735–739, 2016.
- [138] H. Chang, D.-Y. Yeung, and Y. Xiong, "Super-resolution through neighbor embedding," in *Proceedings of the 2004 IEEE Computer Society Conference on Computer Vision and Pattern Recognition, 2004. CVPR 2004.*, vol. 1, pp. I–I, IEEE, 2004.
- [139] D. Cheng-Zhi, T. Wei, C. Pan, W. Sheng-Qian, Z. Hua-Sheng, and H. Sai-Feng, "Infrared image super-resolution via locality-constrained group sparse model," *Acta Physica Sinica*, vol. 63, no. 4, 2014.
- [140] X. Yang, W. Wu, H. Hua, and K. Liu, "Infrared image recovery from visible image by using multi-scale and multi-view sparse representation," in *2015 11th International Conference on Signal-Image Technology & Internet-Based Systems (SITIS)*, pp. 554–559, IEEE, 2015.
- [141] X. Yang, W. Wu, K. Liu, W. Chen, P. Zhang, and Z. Zhou, "Multi-sensor image super-resolution with fuzzy cluster by using multi-scale and multi-view sparse coding for infrared image," *Multimedia Tools and Applications*, vol. 76, no. 23, pp. 24871–24902, 2017.

- [142] E. Zou, B. Lei, N. Jing, and H. Tan, "A super-resolution reconstruction algorithm of infrared pedestrian images via compressed sensing," in *Real-time Photonic Measurements, Data Management, and Processing III*, vol. 10822, pp. 106–111, SPIE, 2018.
- [143] X. Yang, W. Wu, K. Liu, K. Zhou, and B. Yan, "Fast multisensor infrared image super-resolution scheme with multiple regression models," *Journal of Systems Architecture*, vol. 64, pp. 11–25, 2016.
- [144] Y. Wang, L. Wang, B. Liu, and H. Zhao, "Research on blind super-resolution technology for infrared images of power equipment based on compressed sensing theory," *Sensors*, vol. 21, no. 12, p. 4109, 2021.
- [145] Z. Chen, B. Guo, Q. Zhang, and C. Li, "Infrared image super-resolution reconstruction via sparse representation," in *Journal of Physics: Conference Series*, vol. 1069, p. 012171, IOP Publishing, 2018.
- [146] F. Alonso-Fernandez, R. A. Farrugia, and J. Bigun, "Iris super-resolution using iterative neighbor embedding," in *Proceedings of the IEEE Conference on Computer Vision and Pattern Recognition Workshops*, pp. 153–161, 2017.
- [147] S. Ahmadi, P. Burgholzer, P. Jung, G. Caire, and M. Ziegler, "Super resolution laser line scanning thermography," *Optics and Lasers in Engineering*, vol. 134, p. 106279, 2020.
- [148] X. Liu, Y. Chen, Z. Peng, J. Wu, and Z. Wang, "Infrared image super-resolution reconstruction based on quaternion fractional order total variation with lp quasinorm," *Applied Sciences*, vol. 8, no. 10, p. 1864, 2018.
- [149] S. Chen, G. Fan, T. Zhang, and D. Liu, "Research on super-resolution reconstruction algorithm of infrared images of compressive coded aperture," in *Second Symposium on Novel Technology of X-Ray Imaging*, vol. 11068, pp. 514–520, SPIE, 2019.
- [150] J. Liu, S. Dai, Z. Guo, and D. Zhang, "An improved pocs super-resolution infrared image reconstruction algorithm based on visual mechanism," *Infrared Physics & Technology*, vol. 78, pp. 92–98, 2016.
- [151] Y. Hui, C. Fu-Sheng, Z. Zhijie, and W. Chen-Sheng, "A novel regularized adaptive edge-preserving image super-resolution algorithm," *Infrared Millim Waves*, vol. 1, pp. 98–105, 2014.
- [152] J. Dijk, A. W. van Eekeren, K. Schutte, D.-J. J. de Lange, and L. J. van Vliet, "Performance study on point target detection using super-resolution reconstruction," in *Automatic Target Recognition XIX*, vol. 7335, pp. 202–209, SPIE, 2009.
- [153] H. Yu, F.-s. Chen, Z.-j. Zhang, and C.-s. Wang, "Single infrared image super-resolution combining non-local means with kernel regression," *Infrared Physics & Technology*, vol. 61, pp. 50–59, 2013.
- [154] P. Wang, H. Yao, G. Zhang, Y. Kong, S. Lu, and X. Peng, "Land cover target mapping at subpixel scale for landsat 8 oli image by using multiscale-infrared information," *International Journal of Remote Sensing*, vol. 42, no. 3, pp. 1054–1076, 2021.
- [155] C. Dong, C. C. Loy, and X. Tang, "Accelerating the super-resolution convolutional neural network," in *European conference on computer vision*, pp. 391–407, Springer, 2016.
- [156] J. Kim, J. K. Lee, and K. M. Lee, "Accurate image super-resolution using very deep convolutional networks," in *Proceedings of the IEEE conference on computer vision and pattern recognition*, pp. 1646–1654, 2016.
- [157] B. Lim, S. Son, H. Kim, S. Nah, and K. Mu Lee, "Enhanced deep residual networks for single image super-resolution," in *Proceedings of the IEEE conference on computer vision and pattern recognition workshops*, pp. 136–144, 2017.
- [158] X. Wang, K. Yu, S. Wu, J. Gu, Y. Liu, C. Dong, Y. Qiao, and C. Change Loy, "Esrgan: Enhanced super-resolution generative adversarial networks," in *Proceedings of the European conference on computer vision (ECCV) workshops*, pp. 0–0, 2018.
- [159] Y. Huang, Z. Jiang, Q. Wang, Q. Jiang, and G. Pang, "Infrared image super-resolution via heterogeneous convolutional wgan," in *Pacific Rim International Conference on Artificial Intelligence*, pp. 461–472, Springer, 2021.
- [160] K. Fan, K. Hong, and F. Li, "Infrared image super-resolution via progressive compact distillation network," *Electronics*, vol. 10, no. 24, p. 3107, 2021.
- [161] Y. Zou, L. Zhang, C. Liu, B. Wang, Y. Hu, and Q. Chen, "Super-resolution reconstruction of infrared images based on a convolutional neural network with skip connections," *Optics and Lasers in Engineering*, vol. 146, p. 106717, 2021.
- [162] A. Kwasińska, J. Ruminski, M. Szankin, and M. Kaczmarek, "Super-resolved thermal imagery for high-accuracy facial areas detection and analysis," *Engineering Applications of Artificial Intelligence*, vol. 87, p. 103263, 2020.
- [163] H. M. Patel, V. M. Chudasama, K. Prajapati, K. P. Upla, K. Raja, R. Ramachandra, and C. Busch, "Thermisrnet: an efficient thermal image super-resolution network," *Optical Engineering*, vol. 60, no. 7, p. 073101, 2021.
- [164] Y. Zou, L. Zhang, Q. Chen, B. Wang, Y. Hu, and Y. Zhang, "An infrared image super-resolution imaging algorithm based on auxiliary convolution neural network," in *Optics Frontier Online 2020: Optics Imaging and Display*, vol. 11571, pp. 335–340, SPIE, 2020.
- [165] N. Oz, N. Sochen, O. Markovich, Z. Halamish, L. Shpialter-Karol, and I. Klapp, "Rapid super resolution for infrared imagery," *Optics Express*, vol. 28, no. 18, pp. 27196–27209, 2020.
- [166] B. Wang, Y. Zou, L. Zhang, Y. Li, Q. Chen, and C. Zuo, "Multimodal super-resolution reconstruction of infrared and visible images via deep learning," *Optics and Lasers in Engineering*, vol. 156, p. 107078, 2022.
- [167] I. Goodfellow, J. Pouget-Abadie, M. Mirza, B. Xu, D. Warde-Farley, S. Ozair, A. Courville, and Y. Bengio, "Generative adversarial networks," *Communications of the ACM*, vol. 63, no. 11, pp. 139–144, 2020.
- [168] C. Ma, Y. Rao, Y. Cheng, C. Chen, J. Lu, and J. Zhou, "Structure-preserving super resolution with gradient guidance," in *Proceedings of the IEEE/CVF conference on computer vision and pattern recognition*, pp. 7769–7778, 2020.
- [169] I. Gulrajani, F. Ahmed, M. Arjovsky, V. Dumoulin, and A. C. Courville, "Improved training of wasserstein gans," *Advances in neural information processing systems*, vol. 30, 2017.
- [170] B. SHAO, X. TANG, L. JIN, and Z. Li, "Single frame infrared image super-resolution algorithm based on generative adversarial nets," *Journal of Infrared and Millimeter Wave*, vol. 37, no. 4, pp. 427–432, 2018.
- [171] C. Zhang, H. Zhang, and Z. Jiang, "Single infrared remote sensing image super-resolution via supervised deep learning," in *Image and Signal Processing for Remote Sensing XXVI*, vol. 11533, pp. 241–249, SPIE, 2020.
- [172] Z. Li, J. Yang, Z. Liu, X. Yang, G. Jeon, and W. Wu, "Feedback network for image super-resolution," in *Proceedings of the IEEE/CVF conference on computer vision and pattern recognition*, pp. 3867–3876, 2019.
- [173] R. E. Rivadeneira, A. D. Sappa, B. X. Vintimilla, and R. Hammoud, "A novel domain transfer-based approach for unsupervised thermal image super-resolution," *Sensors*, vol. 22, no. 6, p. 2254, 2022.
- [174] G. Batchuluun, J. K. Kang, D. T. Nguyen, T. D. Pham, M. Arsalan, and K. R. Park, "Deep learning-based thermal image reconstruction and object detection," *IEEE Access*, vol. 9, pp. 5951–5971, 2020.
- [175] M. Mostofa, S. N. Ferdous, and N. M. Nasrabadi, "A joint cross-modal super-resolution approach for vehicle detection in aerial imagery," in *Artificial Intelligence and Machine Learning for Multi-Domain Operations Applications II*, vol. 11413, pp. 184–194, SPIE, 2020.
- [176] R. E. Rivadeneira, A. D. Sappa, and B. X. Vintimilla, "Thermal image super-resolution: A novel architecture and dataset," in *VISGRAPP (4: VISAPP)*, pp. 111–119, 2020.
- [177] Y. Wu, L. Cheng, T. Wang, and H. Wu, "Infrared and visible light dual-camera super-resolution imaging with texture transfer network," *Signal Processing: Image Communication*, vol. 108, p. 116825, 2022.
- [178] A. R. Weiß, U. Adomeit, P. Chevalier, S. Landeau, P. Bijl, F. Champagnat, J. Dijk, B. Göhler, S. Landini, J. P. Reynolds, *et al.*, "A standard data set for performance analysis of advanced ir image processing techniques," in *Infrared Imaging Systems: Design, Analysis, Modeling, and Testing XXIII*, vol. 8355, pp. 354–363, SPIE, 2012.
- [179] J. Du, H. Zhou, K. Qian, W. Tan, Z. Zhang, L. Gu, and Y. Yu, "Rgb-ir cross input and sub-pixel upsampling network for infrared image super-resolution," *Sensors*, vol. 20, no. 1, p. 281, 2020.
- [180] S. Khan, M. Naseer, M. Hayat, S. W. Zamir, F. S. Khan, and M. Shah, "Transformers in vision: A survey," *ACM computing surveys (CSUR)*, vol. 54, no. 10s, pp. 1–41, 2022.
- [181] X. Wu, B. Zhou, X. Wang, J. Peng, P. Lin, R. Cao, and F. Huang, "Swinipisr: A super-resolution method for infrared polarization imaging sensors via swin transformer," *IEEE Sensors Journal*, 2023.
- [182] F. Qin, K. Yan, C. Wang, R. Ge, Y. Peng, and K. Zhang, "Lkformer: large kernel transformer for infrared image super-resolution," *Multimedia Tools and Applications*, pp. 1–15, 2024.
- [183] Y. Jiang, Y. Liu, W. Zhan, Y. Tang, J. Li, and Y. Liu, "Cross-modal texture transformer for thermal infrared reference-based super-resolution reconstruction," *Optics & Laser Technology*, vol. 176, p. 110914, 2024.
- [184] S. Liang, K. Song, W. Zhao, S. Li, and Y. Yan, "Dasr: Dual-attention transformer for infrared image super-resolution," *Infrared Physics & Technology*, vol. 133, p. 104837, 2023.
- [185] F. Alonso-Fernandez, R. A. Farrugia, and J. Bigun, "Eigen-patch iris super-resolution for iris recognition improvement," in *2015 23rd*

- European Signal Processing Conference (EUSIPCO)*, pp. 76–80, IEEE, 2015.
- [186] Y. Liu, X. Chen, J. Cheng, H. Peng, and Z. Wang, “Infrared and visible image fusion with convolutional neural networks,” *International Journal of Wavelets, Multiresolution and Information Processing*, vol. 16, no. 03, p. 1850018, 2018.
- [187] Y. Zhang, L. Zhang, X. Bai, and L. Zhang, “Infrared and visual image fusion through infrared feature extraction and visual information preservation,” *Infrared Physics & Technology*, vol. 83, pp. 227–237, 2017.
- [188] Z. Wang, A. C. Bovik, H. R. Sheikh, and E. P. Simoncelli, “Image quality assessment: from error visibility to structural similarity,” *IEEE transactions on image processing*, vol. 13, no. 4, pp. 600–612, 2004.
- [189] Z. Wang, A. C. Bovik, and L. Lu, “Why is image quality assessment so difficult?,” in *2002 IEEE International conference on acoustics, speech, and signal processing*, vol. 4, pp. IV–3313, IEEE, 2002.
- [190] H. R. Sheikh, M. F. Sabir, and A. C. Bovik, “A statistical evaluation of recent full reference image quality assessment algorithms,” *IEEE Transactions on image processing*, vol. 15, no. 11, pp. 3440–3451, 2006.
- [191] Z. Wang and A. C. Bovik, “Mean squared error: Love it or leave it? a new look at signal fidelity measures,” *IEEE signal processing magazine*, vol. 26, no. 1, pp. 98–117, 2009.
- [192] A. Mittal, R. Soundararajan, and A. C. Bovik, “Making a “completely blind” image quality analyzer,” *IEEE Signal processing letters*, vol. 20, no. 3, pp. 209–212, 2012.
- [193] R. Zhang, P. Isola, A. A. Efros, E. Shechtman, and O. Wang, “The unreasonable effectiveness of deep features as a perceptual metric,” in *Proceedings of the IEEE conference on computer vision and pattern recognition*, pp. 586–595, 2018.
- [194] T. Sun, Z. Xiong, Z. Wei, and Z. Wang, “Infrared image super-resolution method for edge computing based on adaptive nonlocal means,” *The Journal of Supercomputing*, vol. 78, no. 5, pp. 6717–6738, 2022.
- [195] A. Mittal, A. K. Moorthy, and A. C. Bovik, “No-reference image quality assessment in the spatial domain,” *IEEE Transactions on image processing*, vol. 21, no. 12, pp. 4695–4708, 2012.
- [196] R. Rombach, A. Blattmann, D. Lorenz, P. Esser, and B. Ommer, “High-resolution image synthesis with latent diffusion models,” in *Proceedings of the IEEE/CVF Conference on Computer Vision and Pattern Recognition*, pp. 10684–10695, 2022.
- [197] T. Salimans and J. Ho, “Progressive distillation for fast sampling of diffusion models,” *arXiv preprint arXiv:2202.00512*, 2022.
- [198] Z. Lyu, X. Xu, C. Yang, D. Lin, and B. Dai, “Accelerating diffusion models via early stop of the diffusion process,” *arXiv preprint arXiv:2205.12524*, 2022.
- [199] H. Cao, C. Tan, Z. Gao, G. Chen, P.-A. Heng, and S. Z. Li, “A survey on generative diffusion model,” *arXiv preprint arXiv:2209.02646*, 2022.
- [200] P. L. Suárez, D. Carpio, and A. D. Sappa, “Enhancement of guided thermal image super-resolution approaches,” *Neurocomputing*, vol. 573, p. 127197, 2024.
- [201] W. Zhang, G. Shi, Y. Liu, C. Dong, and X.-M. Wu, “A closer look at blind super-resolution: Degradation models, baselines, and performance upper bounds,” in *Proceedings of the IEEE/CVF Conference on Computer Vision and Pattern Recognition*, pp. 527–536, 2022.
- [202] X. Li, C. Chen, X. Lin, W. Zuo, and L. Zhang, “From face to natural image: Learning real degradation for blind image super-resolution,” *arXiv preprint arXiv:2210.00752*, 2022.
- [203] F. Yang, H. Yang, Y. Zeng, J. Fu, and H. Lu, “Degradation-guided meta-restoration network for blind super-resolution,” *arXiv preprint arXiv:2207.00943*, 2022.
- [204] Y. Zhou, C. Lin, D. Luo, Y. Liu, Y. Tai, C. Wang, and M. Chen, “Joint learning content and degradation aware feature for blind super-resolution,” in *Proceedings of the 30th ACM International Conference on Multimedia*, pp. 2606–2616, 2022.
- [205] S. Lee, S. Ahn, and K. Yoon, “Learning multiple probabilistic degradation generators for unsupervised real world image super resolution,” *arXiv preprint arXiv:2201.10747*, 2022.
- [206] Y. Huang, Q. Wang, and S. Omachi, “Rethinking degradation: Radiograph super-resolution via aid-srgan,” *arXiv preprint arXiv:2208.03008*, 2022.
- [207] S. Son, J. Kim, W.-S. Lai, M.-H. Yang, and K. M. Lee, “Toward real-world super-resolution via adaptive downsampling models,” *IEEE transactions on pattern analysis and machine intelligence*, 2021.
- [208] R. E. Rivadeneira, A. D. Sappa, B. X. Vintimilla, J. Kim, D. Kim, Z. Li, Y. Jian, B. Yan, L. Cao, F. Qi, *et al.*, “Thermal image super-resolution challenge results-pbvs 2022,” in *Proceedings of the*

IEEE/CVF Conference on Computer Vision and Pattern Recognition, pp. 418–426, 2022.

- [209] K. Wang, Q. Sun, Y. Wang, H. Wei, C. Lv, X. Tian, and X. Liu, “Cippsrnet: A camera internal parameters perception network based contrastive learning for thermal image super-resolution,” in *Proceedings of the IEEE/CVF Conference on Computer Vision and Pattern Recognition*, pp. 342–349, 2022.



Yongsong Huang (Student Member, IEEE) received his B.E. and M.E. degrees from Guilin University of Electronic Technology in 2018 and 2021, respectively. He is currently pursuing a Ph.D. degree in communication engineering at the IIC Laboratory, Tohoku University, Japan, where he serves as a JSPS Research Fellow. He is also a visiting researcher at Harvard University, Massachusetts General Hospital, and National Taiwan University. He co-authored the book “Applications of Generative AI”, published by Springer. In 2024, he was awarded the JSPS Special Research Grant Allowance. His research interests include computer vision, image processing, and super-resolution.



Tomo Miyazaki (Member, IEEE) received B.E. and Ph.D. degrees from Yamagata University and Tohoku University in 2006 and 2011, respectively. He worked on a Geographic Information System at Hitachi, Ltd until 2013. He was a postdoctoral researcher and an assistant professor from 2013 to 2023 at Tohoku University. Since 2024, he has been an Associate Professor. His research interests include pattern recognition and image processing.



Xiaofeng Liu (Member, IEEE) is an Assistant Professor at Yale, and an Associate Member at the Broad Institute of MIT and Harvard. He is also an affiliate faculty member of the Center for Biomedical Data Science, Yale Institutes for Foundations of Data Science, and Global Health. His Ph.D. was jointly supervised by advisors from University of Chinese Academy of Science and Carnegie Mellon University. He received the B.Eng. and B.A. from the University of Science and Technology of China in 2014. He was a recipient of the Best Paper award of the IEEE ISBA 2018. He is the program committee or reviewer for PAMI, TIP, TNNLS, NeurIPS, ICML, CVPR, ICCV, ECCV, Nat. Com. His research interests are centered around the convergence of trustworthy AI/deep learning, medical imaging, and data science to advance the diagnosis, prognosis, and treatment monitoring of various diseases.



Shinichiro Omachi (Senior Member, IEEE) received the B.E., M.E., and Ph.D. degrees in information engineering from Tohoku University, Japan, in 1988, 1990, and 1993, respectively. He worked as an Assistant Professor at the Education Center for Information Processing, Tohoku University, from 1993 to 1996. Since 1996, he has been affiliated with the Graduate School of Engineering, Tohoku University, where he is currently a Professor. From 2000 to 2001, he was a Visiting Associate Professor at Brown University. His research interests include

pattern recognition, computer vision, image processing, image coding, and parallel processing. He is a member of the Institute of Electronics, Information and Communication Engineers, the Information Processing Society of Japan, among others. He received the IAPR/ICDAR Best Paper Award in 2007, the Best Paper Method Award of the 33rd Annual Conference of the GfKI in 2010, the ICFHR Best Paper Award in 2010, and the IEICE Best Paper Award in 2012. From 2020 to 2021, he was the Vice Chair of the IEEE Sendai Section. He served as the Editor-in-Chief for IEICE Transactions on Information and Systems from 2013 to 2015.

TABLE VIII
ABBREVIATIONS.

Abbreviation	Full name
SR	super-resolution
IR	infrared
HR	high-resolution
LR	low-resolution
JPEG	joint photographic experts group
NUC	non-uniformity correction
IQA	image quality assessment
FLIR	forward-looking infrared
LED	light-emitting diode
CNN	convolutional neural network
GAN	generative adversarial net
WGAN	wasserstein GAN
SRFBN	feedback network for image SR
SRCNN	SR CNN
ResNet	residual network
DCGAN	deep convolution GAN
PSRGAN	progressive SR GAN
CycleGAN	cycle-in-cycle GAN
SRGAN	SR GAN
EO	electro-optical
FFT	fast Fourier transform
FPN	fixed pattern noise
NDTI	normalized difference target index
LCTM	land cover target mapping
PSNR	peak signal-to-noise ratio
SSIM	structural similarity index
MSE	mean square error
NIQE	natural image quality evaluator
NSS	natural scene statistics
LPIPS	perceptual image patch similarity

TABLE IX
NOTATIONS.

Notation	Description
I_{LR}, X	low-resolution image
I_{HR}, I	high-resolution image
\hat{I}, Y	reconstructed image
\mathbb{D}	degradation function
\otimes	convolution operation
k	blur kernel
\downarrow_d	downsampling factor
\mathcal{L}	loss function
Φ	regularization term
λ	punishment parameter
θ, Θ	parameters of model
\mathbb{R}	image patch
$[\Psi_c^l, \Psi^l], [\Phi_c, \Phi]$	dictionary pairs
u, v, \mathcal{Z}	sparse codes
M, N	number of dimensions
i	i th training image
\tilde{R}	estimated residual image
R	true residual image
\mathcal{L}_1	loss functions of forward regression
\mathcal{L}_2	loss functions of inverse regression
$\mathcal{L}_{\text{Sobel}}$	loss functions of Sobel edge detector
G	generator
D	discriminator
I_L	generated low-resolution images
$\mathcal{L}_{\text{WGAN}}$	loss functions of WGAN
E	cross-entropy
p_{data}	input image data distribution
Z	distribution of output fake sample by generator
$d_{\mathcal{KL}}$	\mathcal{KL} distance
∇	gradient operator
α, β, γ	control parameters
Ω, u	ℓ_1 -norm
\mathcal{C}_l	brightness similarity
\mathcal{C}_c	contrast similarity
\mathcal{C}_s	structural similarity
P	phase spectrum
λ_1 & λ_2	eigenvalues
σ_{sum} & σ_{ratio}	pre-defined parameters
ε	constant
e	edges
(\hat{k}, l)	pixel